Astron. Astrophys. 197, 163–181 (1988)

ASTRONOMY AND ASTROPHYSICS

Analysis of C II resonance lines in some main sequence early-type stars*

H. Cugier[1] and J. Hardorp[2]

[1] Wroclaw Astronomical Observatory, PL-51-622 Wroclaw, Kopernika 11, Poland
[2] Astronomy Program, State University of New York at Stony Brook, New York, NY 11794, USA

Received October 9, 1986; accepted November 2, 1987

Summary. An analysis of C II resonance lines at 1335 Å in eight main-sequence stars of spectral types A0 to B3 is performed using IUE archival data released for general use. In order to interpret the observed spectra, both LTE and non-LTE line profiles were computed. In stars with low rotational velocities (Vega, π Cet, τ Her and 1 Her) we obtain logarithmic carbon abundances $\log N(\mathrm{C/H}) = -3.55$ to -3.45 in non-LTE case. LTE analysis indicates lower carbon abundances by about 0.1 dex. Substantial differences are found among the fast rotating stars. In 28 Vul we obtain $\log N(\mathrm{C/H}) = -3.52 \pm 0.20$, whereas ψ^2 Aqr, α Leo and 7 Cep have $\log N(\mathrm{C/H}) = -4.90 \pm 0.20$, -4.32 ± 0.20 and -4.02 ± 0.20, respectively.

Key words: lines: profile – stars: early-type – stars: LTE and non-LTE abundances – UV radiation

1. Introduction

Carbon, nitrogen and oxygen are relatively abundant elements and participate in the hydrogen burning through CNO bi-cycle. However, data on the abundances of these elements in early-type stars are remarkably sparse. One of the reasons is the following. Most of the detectable lines of C I, N I and O I in A-type stars fall in the spectral region $\lambda = 6000$ Å to 10800 Å (cf. Lambert et al., 1982), where photographic observations are difficult. In A0 stars, carbon is predominantly singly ionized, but no C II lines were detected in Vega and Sirius by means of ground-based telescopes. There are no easily observed spectral lines of carbon, nitrogen and oxygen in B9 to B4 stars in the visual and near-infrared regions, especially for stars with high and moderate rotational velocities. The observational problems can partially be solved by making use of UV high resolution data of the C II resonance lines at 1335 Å. Freire Ferrero's (1979) analysis indicates that these lines in Vega can be represented very well by theoretical calculations.

In the present paper we report a detailed analysis of the C II resonance lines at 1335 Å in eight main-sequence stars of spectral types A0 to B3, based on the International Ultraviolet Explorer (IUE) archival data released for general use. Although this analysis is the primary goal of the present investigation, we also discuss the C I lines at 1657 Å, which are clearly seen in IUE spectra of the A and late B-type stars.

The observational material used in this work (Sect. 2) is interpreted by means of LTE (Sect. 3) and non-LTE (Sect. 4) line-profile calculations and discussed in terms of influence of the most important parameters upon the profiles and carbon abundances. A detailed comparison of the synthetic spectra (Sect. 5) with the IUE observations of the investigated stars is made in Sect. 6. Finally, the results are summarized and discussed in Sect. 7.

2. Observational material and its analysis

The program stars include eight main-sequence stars of spectral types A0 to B3. Four of them show low rotational velocity, $V \sin i \leq 20\ \mathrm{km\,s^{-1}}$, whereas the remaining ones have $V \sin i \geq 200\ \mathrm{km\,s^{-1}}$, cf. Table 1, where their HD numbers, spectral types, effective temperature T_{eff}, gravity $\log g$ and projected rotational velocity $V \sin i$ are given. The observational material consists of several high resolution IUE spectra, obtained from the National Space Science Data Center at the NASA Goddard Space Flight Center. Relevant information about the analyzed images is shown in Table 2. We used the IUE reduction programs, developed at Stony Brook, which are based on the IUE SISP procedure.

Recently, Adelman and Leckrone (1986) reported that the typical noise amplitude in well-exposed IUE images is about 7% for individual spectra and about 4% for the mean signal of co-added images. To estimate the accuracy of our spectra we used the following procedure. The average spectrum of α Leo was constructed by co-adding four images listed in Table 2, taking into account small relative velocity shifts between images determined by a cross-correlation method. Adopting this spectrum as the reference one, we get rms noise amplitudes of individual spectra (at λ 1330–1340 Å) shown in Table 2. The same procedure was applied for Vega and π Cet. In the case of 7 Cep, 28 Vul, τ Her, ψ^2 Aqr and 1 Her, for which only single spectra were at our disposal, we combined the signal-to-noise ratio near the C II resonance lines with rms noise amplitude measured at the flux-free wavelength range from $\lambda = 1214$ to 1217 Å, i.e., in the central part of the Ly α line, cf. Table 2. Both these methods applied to Vega, α Leo and π Cet give almost the same results.

IUE images may be compared with Copernicus observations of Vega, α Leo and 1 Her, using 0.2 Å-resolution spectra published by Snow and Jenkins (1977). The Copernicus atlas contains the numbers of photon counts per one integration (13^s.76) of

Send offprint requests to: H. Cugier

* Based on observations by the International Ultraviolet Explorer collected at the USA National Space Science Data Center

Table 1. The program stars

Star	HD	Sp	T_{eff} (K)	log g	$V \sin i$ (km s^{-1})
Vega	172167	A0 V	9660 [1]	3.9 [1]	18 [4]
α Leo	87901	B7 V	12200 [1]	3.6 [2]	260 [5]
7 Cep	204770	B7 V	13100 [2]	3.5 [2]	200 [6]
π Cet	17081	B7 V	13300 [2]	3.5 [2]	18 [7]
28 Vul	196740	B5 IV	14700 [2]	3.9 [2]	332 [7]
τ Her	147394	B5 V	15000 [3]	3.7 [3]	32 [7]
ψ^2 Aqr	219688	B5 V	15100 [2]	4.0 [2]	280 [5]
1 Her	160762	B3 V	18000 [3]	3.7 [3]	11 [7]

References for T_{eff} and log g: [1] Code et al. (1976). [2] From the Strömgren photometry. [3] Heasley and Wolff (1981, 1983). References for $V \sin i$: [4] Milliard et al. (1977). [5] Slettebak (1975). [6] This paper. [7] Hoffleit (1982)

the U2 spectrometer, N_λ, and number of observations, I, averaged together to determine the signal, N_λ. According to Snow and Jenkins, the rms noise amplitude of these data may be estimated as $(N'_\lambda/I)^{1/2}$, where N'_λ is the total observed (i.e., uncorrected) count rate, $N'_\lambda \approx 1.5\, N_\lambda + 40$. From this formula, we obtained rms noise amplitudes equal to 2% and 13% for the continuum and C II line cores, respectively. To establish relative flux scale, we used the following expression $F_\lambda \sim N_\lambda/(\lambda E_\lambda)$, where E_λ is the efficiency of U2 phototube at λ. We adopted E_λ recommended by Upson II (1979). In order to compare Copernicus spectra with IUE observations, the latter were broadened to the effective resolution of the U2 spectrometer. An example of such a comparison is given in Fig. 1, where observations of Vega at the wavelength region from $\lambda = 1330$ to 1340 Å are displayed. As one can see, these spectra show the same C II line profiles within the error limits discussed above. Similar results were obtained for α Leo and 1 Her.

We furthermore compared the IUE images of stars with the same spectral types. For example, T_{eff} and log g of π Cet are

Table 2. Journal of the IUE observations

Star	Image no.	Apert.	U.T.	Date	Exp. time	rms (%)	Observer
			h m		m s		
Vega	SWP 8045	L	17 01	1980 Feb 24	00 14	10	J. B. Lester
	SWP 9918	S	16 04	1980 Aug 26	00 09	10	A.L. Lane
	SWP 11213	L	23 44	1981 Feb 1	00 11	13	A. Slettebak
α Leo	SWP 8648	L	22 23	1980 Apr 3	00 12	11	B.E. Woodgate
	SWP 10379	S	13 17	1980 Oct 15	00 25	10	A. Slettebak
	SWP 19087	L	07 29	1983 Jan 26	00 19	9	G.J. Ferland
	SWP 19236	L	14 42	1983 Feb 11	00 12	13	IUE Obser. Staff
7 Cep	SWP 8922	L	23 42	1980 May 4	04 29	9	R.F. Wing
π Cet	SWP 16246	S	00 46	1982 Feb 4	02 30	8	S.J. Adelman
	SWP 16256	L	23 12	1982 Feb 5	04 00	8	S.J. Adelman
28 Vul	SWP 18017	L	08 21	1982 Aug 20	02 45	10	P.K. Barker
τ Her	SWP 3583	S	09 14	1978 Dec 13	01 40	9	L. Van Kamp
ψ^2 Aqr	SWP 10385	L	07 58	1980 Sep 17	03 39	11	A. Slettebak
1 Her	SWP 5720	S	14 28	1979 July 5	01 19	9	D.S. Leckrone

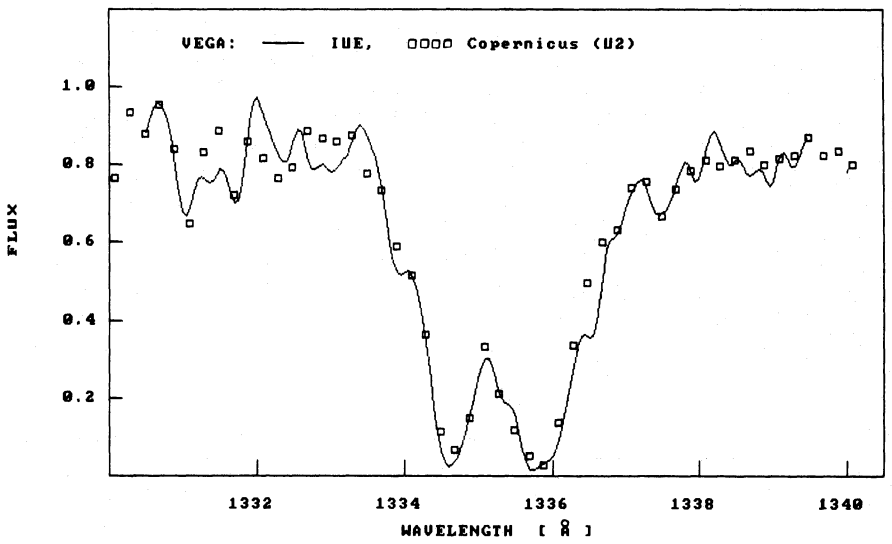

Fig. 1. The C II resonance lines of Vega observed by means of the IUE and Copernicus satellites. The IUE spectrum (SWP 9918) was broadened to the effective resolution (0.2 Å) of the Copernicus U2 spectrometer. Ordinates are in relative fluxes to the continuum

nearly the same as those of α Leo (Table 1). π Cet and α Leo are virtually unreddened ($E(B-V)=0^m.01$ in both cases), with UV flux distributions in agreement with Kurucz's (1979) models for T_{eff} and $\log g$ shown in Table 1. In order to compare high resolution line-spectra of both stars, the spectrum of π Cet was numerically broadened to the rotational velocity of α Leo, i.e., $V \sin i = 260$ km s^{-1}. Figure 2 shows the wavelength region from $\lambda = 1300$ to 1313 Å, where lines of Si II (1304.37 Å and 1309.27 Å) and O I (1304.87 Å and 1306.04 Å) are located (cf. Freire Ferrero, 1979, for a detailed analysis of this spectral region in Vega). We found a similar agreement for all other spectral features at the wavelength region from $\lambda = 1250$ to 1850 Å, with the exception of the C II resonance lines at 1335 Å. As one can see from Fig. 3, the C II lines of α Leo are much weaker than those of π Cet. A similar analysis was performed for other pairs of stars. We found almost the same strength of spectral features at $\lambda = 1300$–1313 Å in 7 Cep and π Cet, while and C II resonance lines are slightly weaker in the case of 7 Cep. The IUE images of 28 Vul and ψ^2 Aqr were compared with SWP 3583 image of τ Her. 28 Vul shows the same strength of the C II and other lines as τ Her does, but the C II lines of ψ^2 Aqr are abnormally weak (see also Hardorp et al., 1986, where ψ^2 Aqr is compared with HD 21362). The much weaker strength of the C II lines of ψ^2 Aqr and α Leo cannot be an artifact, caused by light from a hypothetical hot companion, because other spectral lines are in good agreement with those observed in other stars with similar atmospheric parameters and rotational velocity. We interpret this effect as produced by different carbon abundances in the investigated stars (cf. Sect. 6).

3. The LTE calculations

LTE spectra were calculated using the grid of line blanketed model atmospheres, published by Kurucz (1979). We adopted the Voigt function, H(a, v), as the profile of the line absorption coefficients. The parameters a and v were calculated taking into account the following broadening mechanisms: natural (Γ_R), Doppler due to thermal and microturbulent (ξ) motions of atoms, Stark (Γ_S) and van der Waals (Γ_W). Continuous absorp-

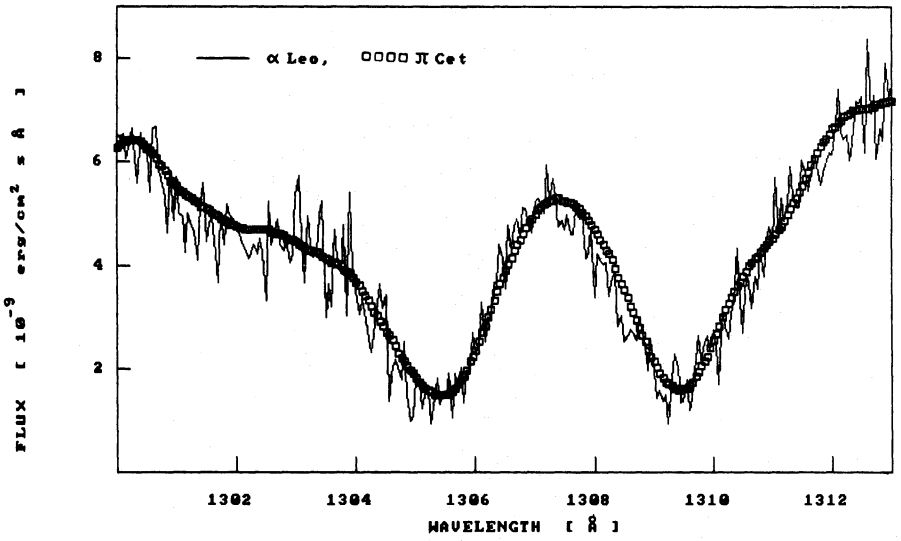

Fig. 2. IUE observations of α Leo (SWP 19236) at the wavelength region from λ 1300 to 1313 Å in comparison with those of π Cet (SWP 16246). The observed spectrum of π Cet was broadened to the rotational velocity of 260 km/s. Ordinates are in absolute flux units of α Leo measured by SWP camera

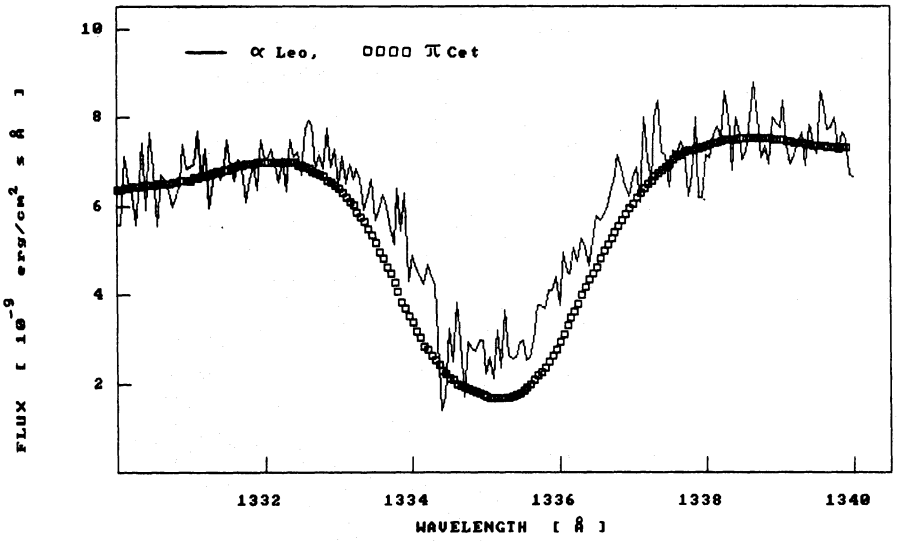

Fig. 3. The same as Fig. 2, but C II resonance lines are shown

tion coefficients and partition functions were adopted from Kurucz (1970). For models with $T_{\rm eff} \leq 13000$ K we also included the Ly α line as a background opacity source near 1335 Å, after Hubeny (1980, 1981) where the importance of the Ly α line in atmospheres of A0 V type stars is discussed. Rayleigh scattering cross-sections were taken from Gavrila (1967), and the Stark broadening of Ly α given by Vidal et al. (1973) was used.

3.1. Atomic data concerning C II and C I lines

For the resonance C II lines we use here theoretical values of f_{ij} and A_{ji} given by Nussbaumer and Storey (1981), cf. Table 3. These values are in good agreement with the theoretical ones of Lennon et al. (1985), as well as with the experimental values. We adopted Stark broadening values from Sahal-Bréchot and Segre (1971) which have an estimated accuracy of 30%. The van der Waals effect was calculated according to the Unsöld and Weidemann's (1955) approximation.

For the C I lines at 1657 Å we adopted theoretical atomic data calculated by Nussbaumer and Storey (1984), cf. Table 3. The damping constants of the Stark effect were taken from Griem (1974), whereas the van der Waals broadening was estimated as described in Sect. 5.

3.2. Discussion of the C II lines at 1335 Å

To assess the sensitivity of the C II lines to the parameters entering the calculations, we analysed the total equivalent widths, W_λ, of these lines at the wavelength range from $\lambda = 1330$ to 1340 Å for several models. The LTE line profiles are rather insensitive to $T_{\rm eff}$, $\log g$ and ξ for $9500 \leq T_{\rm eff} \leq 18000$ K and $3.5 \leq \log g \leq 4.5$, namely: $\Delta T_{\rm eff} = \pm 500$ K gives $\pm 2\%$ in W_λ, which corresponds to $\Delta \log N({\rm C/H}) = \pm 0.02$ dex.; $\Delta \log g = \pm 0.25$ gives $\pm 5\%$ in W_λ ($\Delta \log N({\rm C/H}) = \pm 0.06$ dex.); an increase in microturbulent velocity from 1.5 km s^{-1} to 2.5 km s^{-1} causes an effect of about 2% in W_λ. We also varied other parameters that enter the calculations. The following reasoning illustrates the choice of parameters that we have varied. The C II lines investigated are located on the damping part of the curve of growth. The equivalent width is therefore approximately proportional to $(a\,\beta_0)^{1/2}$ (cf. Mihalas, 1978), where $a = \Gamma/4\pi\Delta\nu_{\rm D}$ with $\Gamma = \Gamma_{\rm R} + \Gamma_{\rm S} + \Gamma_{\rm W}$ (cf. Sect. 3.1), and β_0 is the ratio of the line absorption coefficient at the line center to the continuous absorption coefficient. For all models used in this paper $\Gamma_{\rm W}$ is significantly smaller than $\Gamma_{\rm R}$ and $\Gamma_{\rm S}$. Using a model with $T_{\rm eff} = 13000$ K and $\log g = 4.0$ as reference, we found that if the Sahal-Bréchot and Segre's (1971) $\Gamma_{\rm S}$-values were reduced by one order of magnitude, W_λ decreased by about 14%. This decrease corresponds to $\Delta \log N({\rm C/H}) = -0.18$ dex. The damping wings of the C II lines are mainly due to the natural broadening. The Nussbaumer and Storey (1981) f_{ij} and A_{ji}-values multiplied by 0.7 give W_λ smaller by 19.6% ($\Delta \log N({\rm C/H}) = -0.254$ dex.). We also examined the influence of the computed continua on W_λ. In addition to hydrogen and helium absorbers, we included metal continua, among which C I and Si I are especially important in A and late-B type stars. The C I and Si I continua influence the model atmospheric structure and the emerging flux distribution mainly in the far UV region. The problem requires a self-consistent non-LTE analysis (cf. Hubeny, 1981 and Snijders 1977). These authors found that, in the region where UV continua originate, non-LTE effects lead to much smaller level populations of C I and Si I than the LTE effects do (cf. also Sect. 4). In order to estimate how this affects W_λ, one can use non-LTE level populations of C I as described in Sect. 4. We obtained less than 1% increase in W_λ. As mentioned above, we also included the long-wavelength wing of Ly α as a background opacity for $T_{\rm eff} \leq 13000$ K. The influence of Ly α on the total equivalent widths of the C II resonance lines, W_λ, is negligible.

Table 3. Atomic data for the C II and C I lines

λ (Å)	g	$E_{\rm exc}$ (cm^{-1})	f_{ij}	A_{ji} (10^8 s^{-1})
C II lines				
1334.53	2	0.	0.129	2.42
1335.66	4	64.	0.0128	0.478
1335.71	4	64.	0.116	2.88
C I lines				
1657.00	5	44.	0.1019	2.476
1657.37	3	16.	0.03383	0.824
1658.11	5	44.	0.03398	1.374
1657.89	3	16.	0.04531	3.299
1656.26	3	16.	0.05678	0.8284
1656.92	1	0.	0.1361	1.102

4. Non-LTE calculations

In the present paper, carbon is treated as a trace element, i.e., the structure of the model atmospheres (taken from Mihalas, 1972; Borsenberger and Gros, 1978; and Kurucz, 1979) is assumed to be unaffected by changes in the level populations of carbon. The problem reduces to computing self-consistently the atomic level populations of carbon and the radiation field in the atmosphere. The solution is obtained by the method of complete linearization of Auer and Mihalas (1969, 1970), modified for trace elements by Auer (1973) and Auer et al. (1972). Our code contains a formalism which allows to take into account overlapping transitions at a given frequency point. As a background opacity we also include the Lyman lines (Ly α to Ly δ) as described in Sect. 3.

An initial solution of the statistical equilibrium and radiative transfer equations was obtained from the equivalent-two-level atom approach (Mihalas, 1978.) This solution was used for starting the complete linearization procedure. The level populations were obtained assuming complete redistribution (CR) of re-emitted photons and neglecting the fine structure splitting of levels. Next, the non-LTE line profiles were recalculated for the level populations obtained with the linearization program and taking into account the Voigt function for the line absorption coefficients with the broadening parameters described in Sect. 3.1. The fine structure splitting of levels was then treated explicitely. Finally, the partial redistribution (PR) effect on the emergent line profiles of the C II resonance multiplet was also estimated.

4.1. Atomic model of carbon

The non-LTE approach requires specification of a model atom in which all relevant transitions are included. As mentioned in

Table 4. The carbon atomic model

Level	Ion	Configuration	E_{exc} (cm^{-1})	g	σ_{ik} Ref.	C_{ik} Ref.
1	C I	$2s^2\ 2p^2\ {}^3P$	0.00	9	[1]	[3]
2		$2s^2\ 2p^2\ {}^1D$	10192.63	5	[1]	[4]
3		$2s^2\ 2p^2\ {}^1S$	21648.01	1	[1]	[4]
4		$2s^2\ 2p3s\ {}^3P^0$	60373.00	9	[2]	[5]
5		$2s^2\ 2p3s\ {}^1P^0$	61981.82	3	[2]	[5]
6		$2s^2\ 2p3s\ {}^3D$	69656.24	15	[2]	[5]
7		$2s^2\ 2p3p\ {}^3S$	70676.25	3	[2]	[5]
8		$2s^2\ 2p^3p\ {}^3P$	71301.41	9	[2]	[5]
9		$2s^2\ 2p3d\ {}^3D^0$	78233.03	15	[2]	[5]
10		$2s^2\ 2p3d\ {}^2P^0$	79242.07	9	[2]	[5]
11	C II	$2s^2\ 2p\ {}^2P^0$	0.00	6	[1]	[3]
12		$2s\ 2p^2\ {}^4P$	43035.51	12	[2]	[5]
13		$2s\ 2p^2\ {}^2D$	74931.11	10	[2]	[5]
14		$2s\ 2p^2\ {}^2S$	96493.74	2	[2]	[5]
15		$2s\ 2p^2\ {}^2P$	110651.76	6	[2]	[5]
16		$2s^2\ 3p\ {}^2P^0$	131731.80	6	[2]	[5]
17	C III	$2s^2\ {}^1S$	0.00	1	[1]	[3]
18		$2s\ 2p\ {}^3P^0$	52419.43	9	[2]	[5]
19	C IV	$2s^2\ 2s\ {}^2S$	0.00	2		

References for the photoionization cross-sections σ_{ik}: [1] Henry (1970), [2] Hofsaess (1979)
References for the collisional ionization cross-sections C_{ik}: [3] Lotz (1968), [4] Peach (1968), [5] Seaton (1962).

Sect. 1, we are mainly interested in the analysis of the C II resonance lines at 1335 Å ($2s^2 2p^2 P^0 - 2s\,2p^2\,{}^2D$ transition) and C I lines at 1657 Å ($2s^2\ 2p^2\ {}^3P$–$2s^2\ 2p3s\ {}^3P^0$). Therefore, the adopted model consists of 10 levels of C I, 6 levels of C II, 2 levels of C III and the ground state of C IV, cf. Table 4 where references for collisional bound-free and photoionization cross-section are also given. In addition, the energy levels of C I and C II with the principal quantum numbers up to $n=10$ were added, assuming their populations being in LTE relative to the ground state of the next ionization stage. In the calculations we included only the ground state of the C IV ion, which is justified by the fact that we did not find any observational evidence for C IV lines in the stars investigated here. In some cases this complex model of the carbon atom may be reduced to a smaller number of levels. In particular, it is possible to neglect the C I levels for an analysis of the C II resonance lines in stars with $T_{\rm eff} \geq 13000$ K (cf. Sect. 4.2).

We adopted oscillator strengths mainly from Nussbaumer and Storey (1981, 1984). For transitions between $2p^2\ {}^3P$, $2p^2\ {}^1D$ and $2p^2\ {}^1S$ levels of C I these data were supplemented from Wiese et al. (1966). For $2s^2\ {}^1S$–$2p\ {}^3P^0$ transition of C III we used Loulergue and Nussbaumer's (1974) data. The collisional excitation cross-sections were taken from Henry et al. (1969) (for transitions between $2p^2\ {}^3P$, $2p^2\ {}^1D$ and $2p^2\ {}^1S$ levels of C I), Hayes and Nussbaumer (1984) (for transitions between $2p\ {}^2P^0$, $2p^2\ {}^2D$, $2p^2\ {}^2S$, $2p^2\ {}^2P$ and $2p^2\ {}^4P$ of C II), and from Herkowitz and Seaton (1973) (for $2s^2\ {}^1S$–$2p\ {}^3P^0$ of C III). All other collisional rates were estimated from oscillator strengths for the corresponding radiative transitions using Van Regemorter's (1962) formula. Fifteen most important transitions (viz., bound-free: 1–11, 2–11, 3–11, 11–17, 13–18; bound-bound: 1–4, 1–9, 1–10, 2–5, 3–5, 11–13, 11–14, 11–15, 13–16, 14–16, cf. Table 4) were selected for the linearization procedure. Another bound-free and permitted bound-bound transitions were included with the fixed radiative rates during iterations. The fixed rates were calculated by assuming the radiation field intensity to be constant and equal to the Planck function with radiation temperature T_r. We adopted T_r equal to the local electron temperature at the depths where the line cores are optically thick, and $T_r = T_e$ ($\tau_0^L = 0.73$) for an optically thin region. The boundaries between these regions were determined under the LTE approximation.

4.2. *Level populations*

The level populations of carbon are discussed in terms of the departure coefficients $b_i = N_i/N_i^*$, where N_i and N_i^* are non-LTE and LTE populations of level i, respectively. Figure 4 show examples of the b-factors of C I calculated for Borsenberger and Gros (1978) model atmospheres using the complex atomic model of carbon described in Sect. 4.1. The mass depths where the bound-free transitions (just shortward of the relevant discontinuities) from the ground configuration levels of C I (^3P, ^1D and ^1S) and the cores of the C I 1657 Å lines become optically thin are also indicated. The behaviour of the b-factors shown in Fig. 4 is quantitatively the same as discussed in detail by Snijders (1977) and Hubeny (1981). The underpopulation of the C I levels is the result of photoionizations from the ground-configuration levels of ^3P, ^1D and ^1S, for which the ionization edges are located at $\lambda = 1101$, 1240 and 1444 Å, respectively. Special care was taken to include enough frequency points in the Lyman lines for accurate calculations of the relevant photoionization and recombination

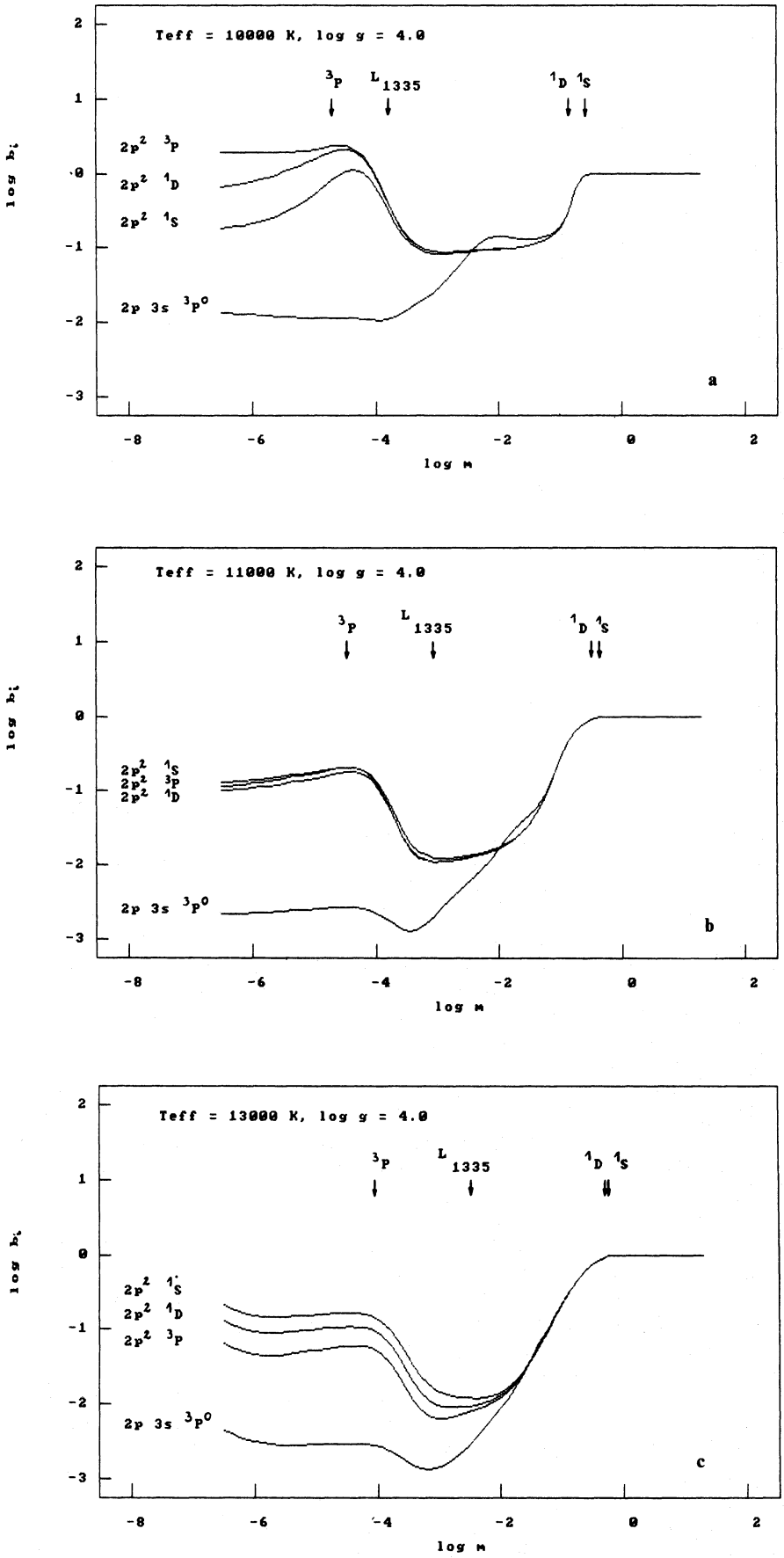

Fig. 4a–c. The *b*-factors of the C I levels calculated using Borsenberger and Gros (1978) model atmospheres with $T_{\rm eff}=10000$ K **a**), 11000 K **b**)and 13000 K **c**), respectively. The arrows indicate the depths where the bound-free transitions from the ground configuration levels of C I (^3P, ^1D and ^1S) and the cores of the C I 1657 Å lines become optically thin

rates. Collisional coupling between ground-configuration levels weakens the depopulation mechanism, but in models corresponding to A0 and the coolest B stars the radiation field at $\lambda < 1240$ Å is significantly reduced by the Lyman lines and, as pointed out by Snijders (1977) and Hubeny (1981), the underpopulation of ^3P and ^1D levels is a result of the collisional coupling with ^1S level.

The *b*-factors of $2s^2\ 2p\ ^2P^0$ and $2s\ 2p^2\ ^2D$ levels of C II corresponding to the resonance multiplet at 1335 Å are shown in Fig. 5. Also shown in this figure are the depths where the Lyman continuum at λ 508 Å (the ionization limit from the ground state of C II, the Balmer continuum at 1335 Å, and the cores of the C II 1335 Å resonance lines become optically thin. The *b*-factors obtained for the complex atomic model of carbon (cf. Sect. 4.1) are shown by means of the solid lines. A Voigt function for the line absorption coefficient of the resonance multiplet at 1335 Å was adopted, whereas a gaussian function was assumed for other bound-bound transitions. The small overpopulation of the C II ground level at mass column densities given by $\log m = -0.8$ to -3.0 shown in Fig. 5a for $T_{\rm eff} = 10000$ K is caused by the significant underpopulation of the C I levels discussed above. This effect is negligible for models with higher effective temperatures, and the C I levels may be neglected in the analysis of the C II resonance lines for stars with $T_{\rm eff} \geq 13000$ K. We furthermore performed several test calculations in order to investigate the sensitivity of the *b*-factors to the adopted atomic model of carbon. For example, the dotted lines shown in Fig. 5 correspond to the case when the simple model of carbon represented by 2 levels of C II plus the corresponding continua was used. As one can see, the coupling of the $2s^2\ 2p\ ^2P^0$ and $2s\ 2p^2\ ^2D$ levels with the higher levels of C II becomes important for atmospheric models with $T_{\rm eff} \geq 13000$ K. In Fig. 5a and b we also plotted (squares) the *b*-factors obtained for the simple model of C II with a gaussian shape for the line absorption coefficient. The resulting level populations differ markedly from those calculated with the Voigt function, which indicates that a proper treatment of the line absorption coefficient is rather necessary for a detailed analysis of the C II line cores. The calculations discussed above were performed for the abundance of carbon equal to $\log N(\mathrm{C/H}) = -3.43$. We also show in Fig. 5 (dashed lines) the *b*-factors obtained for $T_{\rm eff} = 15000$ K with $\log N(\mathrm{C/H}) = -4.43$. The complex atomic model was used.

4.3. *Non-LTE line profiles*

Figure 6 shows an example of the calculated C I line profiles near 1657 Å. As one can see, non-LTE effects lead to a weaker strength of this multiplet in comparison with the LTE calculations. The total equivalent widths, calculated from 1654 Å to 1660 Å, are given in Table 5 for a few model atmospheres. The C I lines at 1657 Å are sensitive to the parameters entering into the calculations, including the abundance of carbon. Both LTE and non-LTE equivalent widths shown in Table 5 were calculated using Kurucz's ($T_{\rm eff} = 9500$ K) and Borsenberger and Gros ($T_{\rm eff} = 10000$, 11000 and 13000 K) model atmospheres.

The non-LTE line profiles of the C II resonance multiplet, calculated from the Borsenberger and Gros (1978) model atmosphere with $T_{\rm eff} = 10000$ K and $\log g = 4.0$ under the assumption of the complete redistribution, are shown in Fig. 7 by means of the continuous line. The line source function tends to be collisionally dominated and small emission features seen in the line cores reflect the radiatively induced temperature rise in the outer layers of a non-LTE, radiative equilibrium model atmosphere (Cayrel effect).

According to Sect. 3, the damping wings of the C II resonance lines are caused in a large part by the natural broadening. This suggests that coherent scattering of photons at the line wings may play some role in forming the emergent line profiles. The angle-averaged redistribution function for a resonance line, transformed to the laboratory frame, can be approximated by:

$$R(\nu', \nu) = \gamma R_{\rm II}(\nu', \nu) + (1-\gamma) R_{\rm III}(\nu', \nu), \tag{1}$$

with $\gamma = (\Gamma_{\rm R} + \Gamma_{\rm I})/(\Gamma_{\rm R} + \Gamma_{\rm I} + \Gamma_{\rm C})$, where $\Gamma_{\rm R}$, $\Gamma_{\rm I}$ and $\Gamma_{\rm C}$ are damping-widths from radiative decays, inelastic collisions, and elastic collisions, respectively (cf. e.g., Mihalas, 1978). The first term in Eq. (1) represents coherent scattering, whereas the second, complete redistribution of the re-emitted photons. Using a model atmosphere with $T_{\rm eff} = 10000$ K and $\log g = 4.0$, we obtained γ from 1.0 (at $\log \tau^{\rm C}_{1335} = -7$) to 0.45 (at $\log \tau^{\rm C}_{1335} = 0$). Similar values were found for other models in this paper using Nussbaumer and Storey's (1981) atomic data, the Stark broadening given by Sahal-Bréchot and Segré (1971) and collisional cross-sections calculated by Hayes and Nussbaumer (1984) and Lennon et al.(1985). In order to estimate the partial redistribution (PR) effect on the emergent line profiles, we used the following approach. It is adequate to adopt $R_{\rm III}(\nu', \nu) = \phi_{\nu'}\phi_{\nu}$, where ϕ_ν is a line absorption coefficient. This assumes that complete redistribution in the atom's frame leads to complete redistribution in the observer's frame. For the far wings we have $R_{\rm II} \rightarrow \phi_\nu \delta(\nu' - \nu)$. If we furthermore neglect the stimulated emission and assume detailed radiative balance for a given line, we obtain the following simple form of the emission coefficient in the case of a two-level atom (cf. e.g., Hubeny, 1981):

$$\eta_\nu = \frac{h\nu}{4\pi}[n_{\rm u} A_{\rm ul} \phi_\nu (1-\gamma^*) + n_{\rm l} B_{\rm lu} \phi_\nu J_\nu \gamma^*], \tag{2}$$

where $\gamma^* = A_{\rm ul}\gamma/(A_{\rm ul} + C_{\rm ul})$; $A_{\rm ul}$ and $B_{\rm lu}$ are the Einstein coefficients, $C_{\rm ul}$ is the downward collisional rate, $n_{\rm l}$ and $n_{\rm u}$ are the populations of the lower and upper levels, respectively, and J_ν is the mean radiation intensity. In model calculations presented here the factor $(h\nu/kT)$ is sufficiently large so that we can neglect stimulated emission. The condition $R_{\rm II} \rightarrow \phi_\nu \delta(\nu' - \nu)$ is satisfied with good precision for $\Delta\lambda > 6\Delta\lambda_{\rm D}$ (cf. Kneer, 1975). (We get $\Delta\lambda > 0.1$ Å for $\Delta\lambda_{\rm D}$ corresponding to $T = 10000$ K). Furthermore, the above-mentioned detailed radiative balance in the C II resonance lines may be safely adopted at mass depths corresponding to $\tau_{\rm L}(\Delta\lambda) = 1$ with $\Delta\lambda \geq 0.1$ Å. The resulting line profiles are shown in Fig. 7 by means of the dotted line. As one can see, PR-effect leads to slightly weaker wings of the C II resonance lines. For a model with $T_{\rm eff} = 10000$ K and $\log g = 4.0$ we obtained a decrease of about 9% in the total equivalent width W_λ, which corresponds to $\Delta \log N(\mathrm{C/H}) = -0.11$ dex. The PR-effect is more important for models with low $\log g$ value due to small electron density in the region of formation of the C II lines. For example, in the case of $T_{\rm eff} = 17500$ K we obtained a decrease in W_λ of the orders of 9% and 18% for $\log g = 4.0$ and 3.0, respectively.

The difference between the C II line profiles, calculated with complete redistribution and with partial redistribution can be easily understood. Under the assumptions mentioned above the line absorption coefficient is equal to $\kappa_\nu = (h\nu/4\pi) B_{\rm lu} n_{\rm l} \phi_\nu$ and the

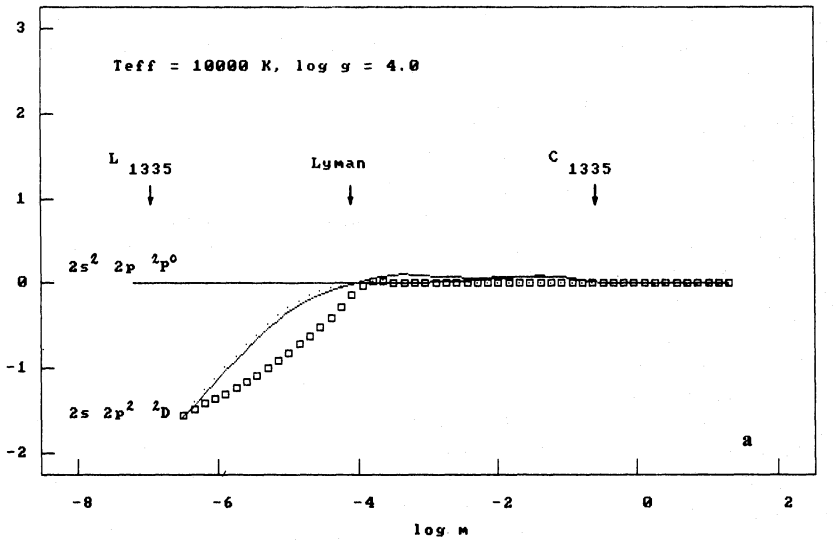

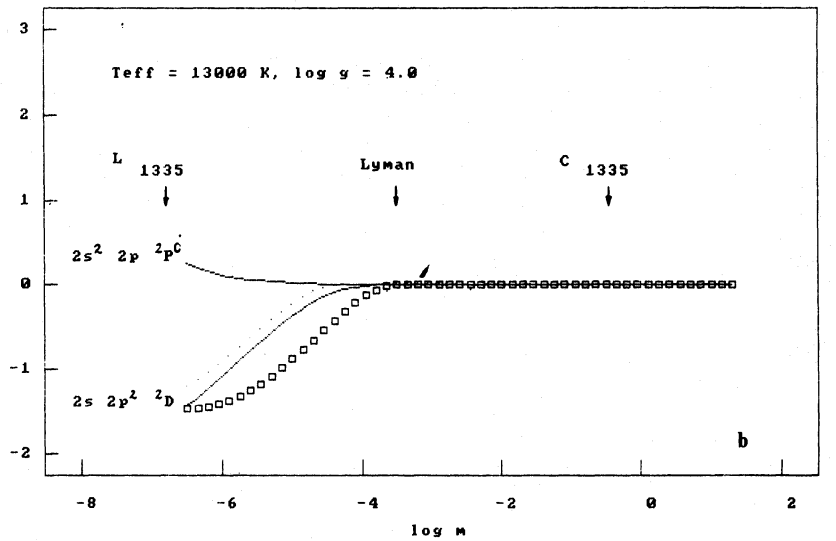

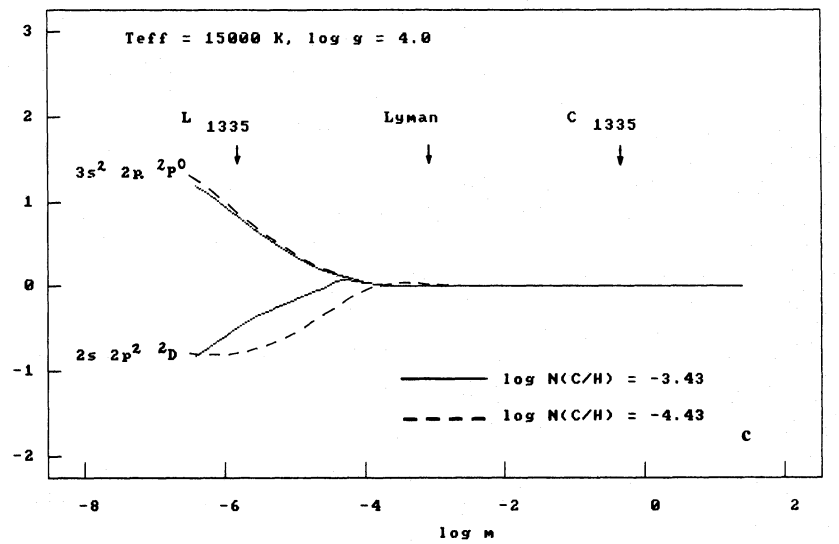

Fig. 5a–e. The *b*-factors of the C II levels corresponding to the resonance multiplet at $\lambda = 1335$ Å, calculated using Borsenberger and Gros (1978) model atmospheres with **a** $T_{\rm eff} = 10000$ K and **b** 13000 K and Mihalas (1972) models with **c** $T_{\rm eff} = 15000$ K and **d**, **e** $T_{\rm eff} = 17500$ K, respectively. Different types of curves illustrate the sensitivity of the *b*-factors to the adopted atomic model of carbon (cf. Sect. 4.2). The arrows indicate the depths where the cores of the C II 1335 Å resonance lines (L_{1335}), the Balmer continuum at 1335 Å (C_{1335}) and the Lyman continuum at 508 Å (Lyman) become optically thin

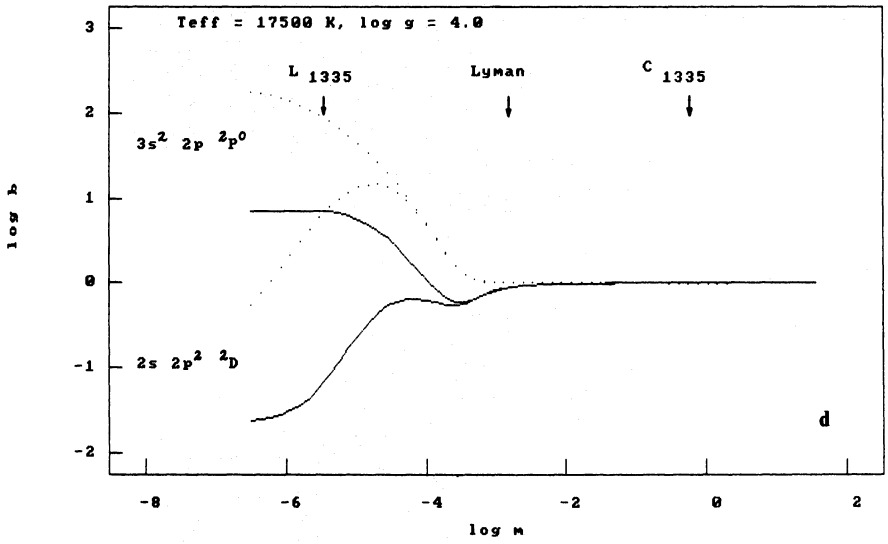

Fig. 5d

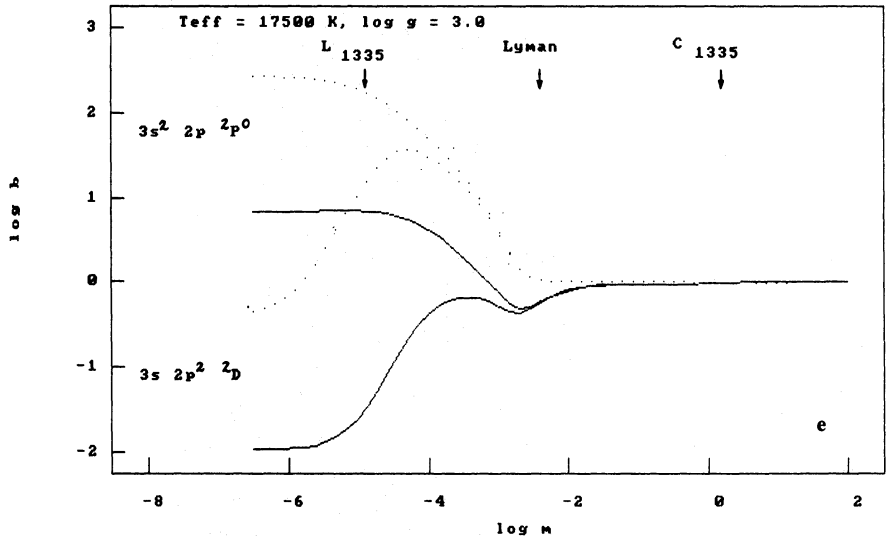

Fig. 5e

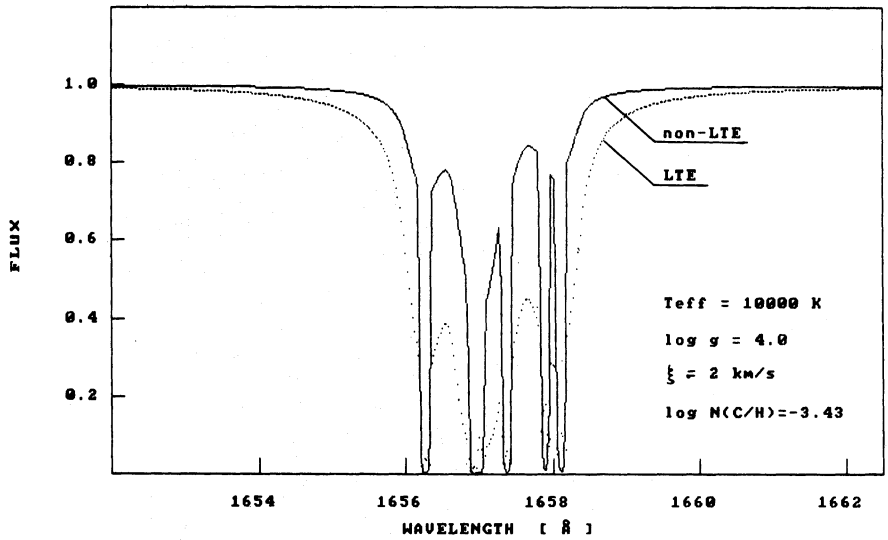

Fig. 6. LTE and non-LTE line profiles of the C I multiplet at 1657 Å calculated using Borsenberger and Gros (1978) model atmosphere of $T_{\rm eff}=10000$ K and $\log g=4.0$. $\log N(\mathrm{C/H})=-3.43$ and $\xi=2\ \mathrm{km\,s^{-1}}$ were assumed. Ordinates are in relative fluxes to the continuum

Table 5. Total equivalent widths of the C I lines at 1657 Å (see Table 3)

$T_{\rm eff}$ (Å)	log g	ξ (km s^{-1})	log N(C/H)	W_λ^a[Å] LTE	non-LTE
9500	4.0	2.0	−3.43	2.43	1.77
10000	4.0	2.0	−3.43	2.15	1.27
10000	4.0	2.0	−3.20	2.55	—
10000	4.0	2.0	−3.70	1.72	—
11000	4.0	2.0	−3.43	1.13	0.70
13000	4.0	2.0	−3.43	0.73	0.60

[a] Calculated from λ 1654.0 to 1660.0 Å

line source function is given by:

$$S_{\nu L}=\frac{\eta_\nu}{\kappa_\nu}=\frac{2h\nu^3}{c^2}\frac{g_l}{g_u}\frac{b_u}{b_i}\frac{N_u^*}{N_l^*}(1.0-\gamma^*)+J_\nu\gamma^*. \quad (3)$$

According to Sect. 4.2 the departure coefficients b_l and b_u are equal to each other in the region where the line wings originate. The first term in Eq. (3) corresponds to the Planck function when the stimulated emission is neglected. Figure 8 shows both the Planck function, B_ν, and the mean intensity of radiation, J_ν, at λ = 1333.5 Å as a function of mass depth for a model atmosphere with $T_{\rm eff}$ = 10000 K and log g = 4.0. The mass depth where the monochromatic (λ = 1333.5 Å) optical depth is equal to 2/3 is also indicated. The wavelength point λ = 1333.5 Å can be regarded as representative for wings of the C II resonance lines. As one can

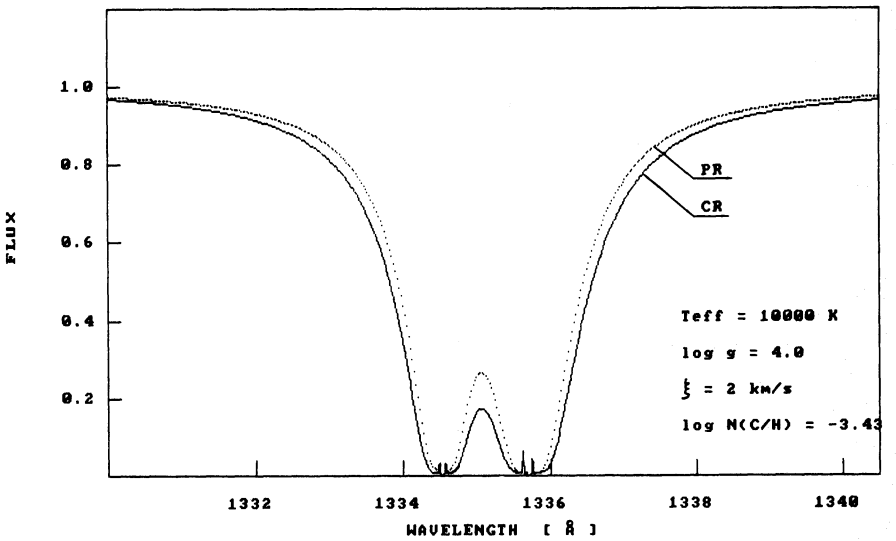

Fig. 7. Non-LTE line profiles of the C II resonance multiplet calculated using a Borsenberger and Gros (1978) model atmosphere of $T_{\rm eff}$ = 10000 K and log g = 4.0. The solid line corresponds to the non-LTE calculations assuming the complete redistribution (CR), whereas the dotted line shows non-LTE calculations with the partial redistribution (PR) effect (see Sect. 4.3). log N(C/H) = −3.43 and ξ = 2 km s^{-1} were adopted. Ordinates are in relative fluxes to the continuum

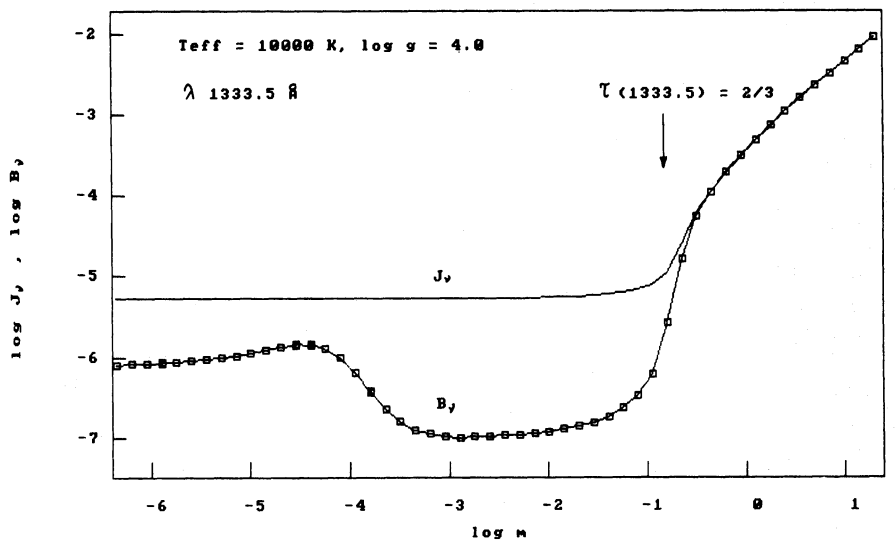

Fig. 8. The monochromatic (λ = 1333.5 Å) mean intensity of radiation, J_ν, and the corresponding Planck function, B_ν, calculated at the C II line wings using a Borsenberger and Gros (1978) model atmosphere of $T_{\rm eff}$ = 10000 K and log g = 4.0. The mass depth, m, where the monochromatic (λ = 1333.5 Å) optical depth, τ, is equal to 2/3 is also indicated

see from Fig. 8, at this optical depth the mean intensity of radiation is greater than the local Planck function. The parameter γ^* in Eq. (2) is equal to 0.67. The line source function with partial redistribution is therefore greater than the source function corresponding to the case of complete redistribution at mass depths of interest. As mentioned above our calculations with partial redistribution (PR) are not valid in the line cores and in the very near line wings, i.e., $\Delta\lambda \leq 6\Delta\lambda_D$. According to Freire Ferrero and Gouttebroze (1985) and Freire Ferrero (1987, personal communication) the PR profiles should be deeper than the CR ones in the line cores. But in practice, the C II line cores have a very low intensity and even if PR line cores are deeper than CR ones, their difference is practically not detected (cf. Freire Ferrero and Gouttebroze, 1985).

We would like to add that the situation is different for the Mg II resonance lines at 2800 Å. The mean intensity of radiation is lower than the corresponding Planck function in the atmospheric depths where the Mg II line wings originate. Therefore, the emergent flux obtained with partial redistribution is lower in comparison with the complete redistribution case. Our test calculations performed for the Mg II line wings are in good agreement with the Freire Ferrero et al. (1983) results.

Finally, as mentioned in Sect. 4.2, most of the non-LTE level populations were calculated assuming the abundance of carbon equal to $\log N(\mathrm{C/H}) = -3.43$. Non-LTE carbon abundances in stars under study (cf. Sect. 6) were determined from line profile calculations using these level populations multiplied by a factor ε, which correspond to a new carbon abundance of $\log N(\mathrm{C/H}) = -3.43 + \log \varepsilon$. Test calculations performed for $T_{\mathrm{eff}} = 15000$ K and $\log g = 4.0$ indicate that this is a good approximation. We obtained $W_\lambda = 1.086$ Å for $\varepsilon = 0.1$, whereas the consistent non-LTE level populations calculated for $\log N(\mathrm{C/H}) = -4.43$ yield $W_\lambda = 1.027$ Å.

5. Synthetic spectra

Synthetic spectra were calculated in the wavelength region around the C II and C I lines discussed in Sects. 3 and 4. We used Kurucz's (1981) atomic data for the Fe II ion; in addition to the gf-values, we adopted his partial sums to estimate the natural, Stark, and van der Waals broadenings. Furthermore, we took into account all spectral lines of the elements with $Z < 28$ at ionization states I–IV, given by Kurucz and Peytremann (1975). For these lines we used the classical vlaue for the natural line broadening. The following Kurucz and Avrett's (1981) formula was adopted for the van der Waals effect:

$$\Gamma_W = 4.5\,10^{-9}(R_u^2)^{0.4}[N_H + 0.42\,N_{He} + 0.85\,N_{H_2}](T/10^3)^{0.3}. \quad (4)$$

This formula was obtained for elements with the atomic weight $A > 4$ by taking into account the polarization of H, He, and H_2. Moreover, it was assumed that the mean-square radius of the lower level, R_l, is small in comparison with the mean-square radius of the upper level, R_u. For the iron group elements, R_u was estimated according to Kurucz and Avrett (1981) as:

$$R_u^2 = \frac{45 - S}{Z_{\mathrm{eff}}},$$

where S is the atomic number of the sequence, i.e., $S = 26$ for the iron sequence, and $Z_{\mathrm{eff}} - 1$ is the charge of ions. For other elements the hydrogenic form was adopted:

$$R_u^2 = 2.5\left(\frac{n_{\mathrm{eff}}}{Z_{\mathrm{eff}}}\right)^2,$$

where n_{eff} is the effective principal quantum number.

We estimated the Stark effect for lines of the ionic species starting with the treatment as in Griem (1968). In Griem's formulation, the width of the Stark broadening is expressed in terms of the Gaunt factors, g, and the transitions to levels interacting with the upper and lower states are taken into account. In the simplest version, the sum over interacting levels can be approximated by including only the nearest strongly interacting level for the upper state, i.e.,

$$\Gamma_S = 8\left(\frac{\pi}{3}\right)^{3/2}\frac{ha_0}{m}\left(\frac{E_H}{kT}\right)^{1/2} N_e\left[R_u^2\bar{g}\left(\frac{3kT}{2\Delta E_u}\right)\right]. \quad (5)$$

Finally, we used the following Freudenstein and Cooper's (1978) formula for the Stark effect of the lines of neutral atoms:

$$\Gamma_S = \frac{1}{2}\frac{ha_0}{m}\left(\frac{E_H}{kT}\right)^{1/2} N_e R_u^2 f(x), \quad (6)$$

where

$$f(x) = e^{-1.33x}\ln\left(1 + \frac{2.27}{x}\right) + \frac{0.487x}{0.513 + x^{5/3}} + \frac{x}{7.93 + x^3}$$

and

$$x = R_u\frac{\Delta E_u}{3kT}.$$

We estimated the energy spacing, ΔE_u, between the upper transition level and the nearest strongly interacting level as $\Delta E_u = \Delta E_\infty/2$, where ΔE_∞ is the ionization energy of the upper level.

In the calculations presented in this paper, the Fe II lines are the most important blends for which the natural broadening is dominant over most of the relevant depth range. We believe that using the above-mentioned Kurucz's (1981) partial sums for Fe II in order to estimate Γ_R-values is more justified than assuming the classical values of the natural line broadening. In order to estimate the accuracy of Γ_S calculated by means of Eqs. (5) and (6), we compared them with the more sophisticated calculations of Griem (1974). We found an agreement within about 50% of UV spectral lines listed by Griem (1974).

6. Comparison with observations

6.1. *Vega*

For the bright star Vega (α Lyr) $T_{\mathrm{eff}} = 9660 \pm 200$ K and $\log g = 3.9 \pm 0.2$ following resp. Code et al. (1976), Dreiling and Bell (1980) and Hubeny (1981). However, slightly lower effective temperature of 9400 K and 9540 ± 275 K were obtained by Kurucz (1979) and Beeckmans (1977), respectively. According to Sect. 4.1, these small discrepancies in T_{eff} are almost unimportant for the LTE analysis of the C II resonance lines and we can adopt for Vega a model with $T_{\mathrm{eff}} = 9500$ K and $\log g = 4.0$ from the Kurucz's (1979) grid of the line-blanketed models.

In the analysis reported here it is necessary to determine the continuum level on the observed spectra. The procedure we used

for stars with low rotational velocities is illustrated in detail for Vega. For this star the local "continuum" level at the wavelength region near the C II resonance lines is influenced by the red wing of the Ly α line, which may be reproduced very well by theoretical predictions (cf. Hubeny, 1981). We calculated emergent fluxes at the wavelength region from $\lambda=1295$ to 1345 Å for several Kurucz's (1979) model atmospheres and compared them with the IUE observations. The best fit is shown in Fig. 9, where the upper line denoted by Ly α corresponds to the calculated red wing of Ly α line for $T_{\rm eff}=9500$ K and $\log g=4.0$. In Fig. 9 we also plotted the LTE synthetic spectrum (dotted line) near the C II lines at 1335 Å, which shows the best agreement with the observations. We obtained $\log N(\mathrm{C/H})=-3.66\pm0.15$. The accuracy of the carbon abundance determination was estimated by taking into account the uncertainties in the following parameters: $\Delta T_{\rm eff}=\pm200$ K, $\Delta\log g=\pm0.2$, $\Delta\xi=\pm2$ km s^{-1}, and an error in the continuum level equal to 10%, which is a typical rms noise amplitude of the IUE spectra (cf. Sect. 2). We would like to add that in the calculations of the synthetic spectra for Vega we used Fe and Ti abundances of Dreiling and Bell (1980), whereas solar abundances listed by Kurucz (1979) were assumed for other blends. A microturbulent velocity equal to 2 km s^{-1} (cf. Dreiling and Bell, 1980) was adopted. Finally, the calculated spectrum was broadened to the rotational velocity of $V\sin i=18$ km s^{-1} (cf. Milliard et al., 1977) and convolved with the instrumental profile, assuming the gaussian shape for the latter with FWHM as in Boggess et al. (1978). The lack of a complete list of spectral lines at the analysed wavelength region is the major source of the discrepancy between the synthetic and observed spectra shown in Fig. 9.

Unfortunately, there were no non-LTE model atmospheres with $T_{\rm eff}=9400$ to 9660 K at our disposal; we used Borsenberger and Gros (1978) model with $T_{\rm eff}=10000$ K and $\log g=4.0$ in our non-LTE analysis of the C II line profiles. Figure 10 shows the non-LTE line profiles, calculated by taking into account partial redistribution effect (cf. Sect. 4.3), together with SWP 9918 image of Vega. The best fit was obtained for $\log N(\mathrm{C/H})=-3.55\pm0.20$. As one can see from Fig. 10, the observed line profiles indicate emission features at the line cores. Such features are not seen in the 0.05 Å-resolution spectra of Vega analysed by Freire Ferrero

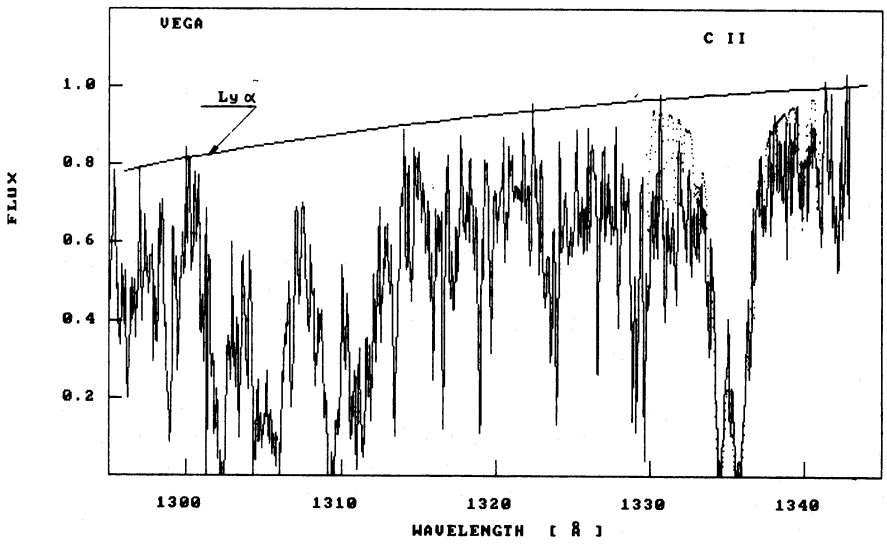

Fig. 9. IUE observations of Vega (SWP 9918) at the wavelength region $\lambda=1295$ Å to 1343 Å. The upper solid line corresponds to the calculated red wing of the Ly α line. The dotted line shows the LTE synthetic spectrum calculated using Kurucz's (1979) model atmosphere of $T_{\rm eff}=9500$ K and $\log g=4.0$. $\log N(\mathrm{C/H})=-3.66$ and $\xi=2$ km s^{-1} were adopted. Ordinates are in relative fluxes normalized near 1350 Å

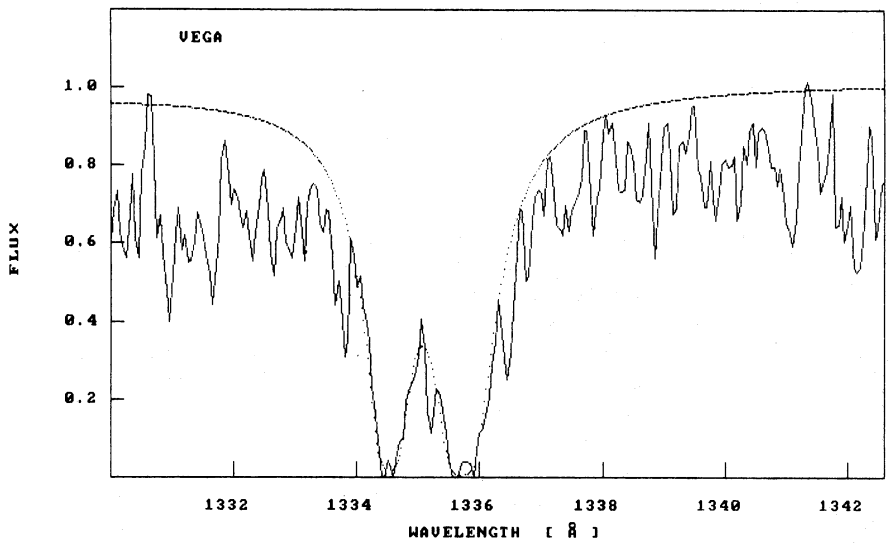

Fig. 10. Comparison of the non-LTE line profiles of the C II resonance multiplet with the SWP 9918 image of Vega. The theoretical profiles were calculated using a Borsenberger and Gros (1978) model atmosphere of $T_{\rm eff}=10000$ K, $\log g=4.0$, $\log N(\mathrm{C/H})=-3.55$, $\xi=2$ km s^{-1} and $V\sin i=18$ km s^{-1}. Ordinates are in relative fluxes normalized near 1350 Å

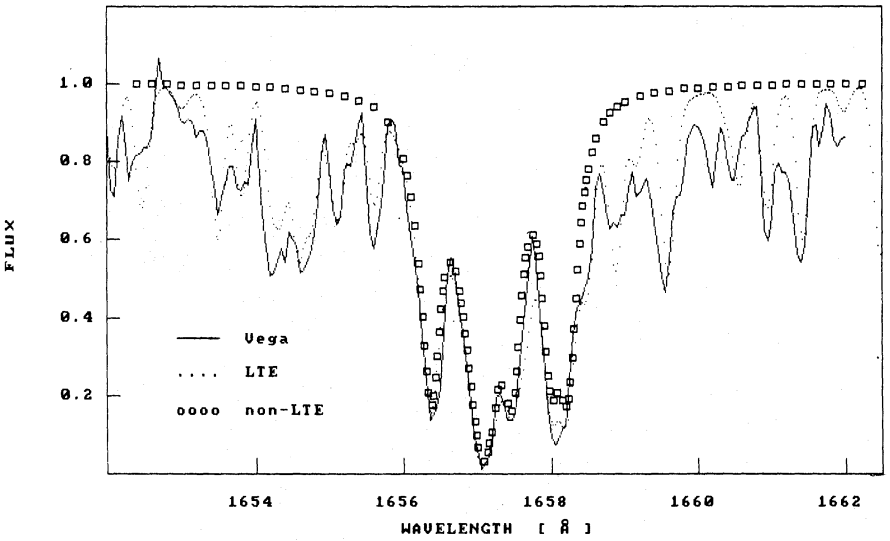

Fig. 11. Comparison of the LTE synthetic spectrum (dots), non-LTE line profiles (squares) of the C I multiplet at 1657 Å with the SWP 9918 image of Vega (solid line). The theoretical spectra were calculated using Kurucz's (1979) model atmosphere of $T_{\rm eff}=9500$ K, $\log g=4.0$, $\xi=2\,{\rm km\,s^{-1}}$ and $V\sin i=18\,{\rm km\,s^{-1}}$. $\log N({\rm C/H})$ equal to -3.60 (LTE) and -3.45 (non-LTE) were obtained

(1979). In our opinion, the observed features at the line cores are most probably caused by some errors in IUE reduction procedure. The spectral features seen at the line cores may also be produced by supplementary absorptions. An inspection of IUE spectra and Copernicus U1 data (cf. Freire Ferrero's Figs. 2 and 4) indicates that several blends (at wavelength region from $\lambda=1332.5$ to 1334 Å and at $\lambda=1336.5$ Å) are much deeper in IUE spectra than in Copernicus U1 data. Finally, we would like to note here that the line source function of the C II resonance multiplet tends to be collisionally dominated for a model corresponding to Vega. A temperature rise in the outer layers may produce emission features at the line cores, but the Cayrel effect is not sufficient to explain the observations (cf. also Freire Ferrero (1979) for a more detailed discussion of this point).

As mentioned in Sect. 1, there are well observed C I lines at 1657 Å. The predicted line profiles are sensitive to the adopted model atmospheres (cf. Sect. 4.3) and the non-LTE model with $T_{\rm eff}=10000$ K has the effective temperature too high to be useful for comparing the calculated C I lines with observations of Vega. Therefore we used an LTE model atmosphere with $T_{\rm eff}=9500$ K and $\log g=4.0$, given by Kurucz (1979), in both the LTE and non-LTE calculations of the C I line profiles. Figure 11 shows the resulting LTE synthetic spectrum (dots) and non-LTE line profiles (squares) in comparison with SWP 9918 image of Vega. The synthetic spectrum was calculated in exactly the same way as described above in the case of the spectra near $\lambda=1335$ Å. We obtained $\log N({\rm C/H})=-3.60$ and -3.45 in the cases of LTE and non-LTE analyses, respectively. The accuracy of these carbon abundance determinations is about ±0.25 dex., taking into account the above given uncertainties in $T_{\rm eff}$, $\log g$ and ξ.

As mentioned above, the C II resonance lines of Vega observed by means of the Copernicus satellite have been already analysed by Freire Ferrero (1979). He found $\log N({\rm C/H})=-3.52$ under the LTE assumption. The discrepancy between Freire Ferrero's and our results (by about 0.14 dex.) may be explained by different f_{ij}- and A_{ji}-values used in these cases: Freire Ferrero's values were about 15% smaller than those of Nussbaumer and Storey's (1981), used in the present paper. The differences in non-LTE calculations may probably be explained as due to different atomic data, model atmospheres, and different computing codes.

Table 6. The derived carbon abundances

	$\log N({\rm C/H})$	
Star	LTE	non-LTE
Vega	-3.66 ± 0.15	-3.55 ± 0.20
α Leo	-4.43 ± 0.15	-4.32 ± 0.20
7 Cep	-4.13 ± 0.15	-4.02 ± 0.20
π Cet	-3.63 ± 0.15	-3.51 ± 0.20
28 Vul	-3.63 ± 0.15	-3.52 ± 0.20
τ Her	-3.60 ± 0.15	-3.45 ± 0.20
ψ^2 Aqr	$-5.0\ \pm0.2$	$-4.9\ \pm0.2$
ι Her	-3.65 ± 0.15	-3.51 ± 0.20

Recently, Lambert et al. (1982) have performed an abundance analysis of C, N and O for Vega, making use of the C I, N I and O I lines located in the visual and near infrared regions. They found $\log N({\rm C/H})=-3.43\pm0.15$, which differs by 0.12 ± 0.25 dex and 0.02 ± 0.29 dex from the carbon abundance obtained by us from the ultraviolet C II and C I lines, respectively. We therefore conclude that the carbon abundances derived from the C II resonance lines at 1335 Å, C I lines located at UV, visual and near infrared regions are the same within error limits set by uncertainties of the atomic data and atmospheric parameters of Vega. The carbon abundance of Vega derived from the C II resonance lines ($\log N({\rm C/H})=-3.55\pm0.20$) is listed in Table 6.

6.2. π Ceti

π Cet is a B7 V star with small rotational velocity, $V\sin i=18\,{\rm km\,s^{-1}}$ (cf. Hoffleit, 1982). We obtained $T_{\rm eff}=13300$ K and $\log g=3.54$ from the Strömgren photometric indices, taken from the Lindemann and Hauck's (1973) catalogue. We used the theoretical grid of m_1 versus c_1 of Relyea and Kurucz (1978), after the observed indices were dereddened by a method for B-type stars, outlined by Crawford (1973). Kurucz's (1979) model with $T_{\rm eff}=13000$ K and $\log g=3.5$ was then selected for calculations

of the LTE synthetic spectra. We obtained an abundance of carbon equal to $\log N(\mathrm{C/H}) = -3.63 \pm 0.15$. For the non-LTE analysis of the C II lines we used Borsenberger and Gros (1979) model with $T_{\mathrm{eff}} = 13000$ K and $\log g = 4.0$. In this case we obtained $\log N(\mathrm{C/H}) = -3.55 \pm 0.20$, but the final non-LTE abundance estimate, shown in Table 6, was corrected to the lower $\log g$ value, corresponding to π Cet. In the calculations we used the Nussbaumer and Storey's (1981) atomic data and the damping constants of the Stark effect given by Sahal-Brechot and Segré (1971). Figure 12 shows the comparison of the LTE and non-LTE spectra with the SWP 16246 image of π Cet.

Both LTE and non-LTE calculations were also performed for C I lines at 1657 Å. We found $\log N(\mathrm{C/H}) = -4.3 \pm 0.25$ and -3.45 ± 0.25 in the case of LTE and non-LTE, respectively. These values differ markedly between each other, which can be explained in terms of LTE and non-LTE level populations of C I discussed in Sect. 4.2. Non-LTE analysis of the C I lines gives almost the same abundance of carbon as derived above from the C II resonance lines. The best fit of the calculated spectra to the SWP 16246 image of π Cet is shown in Fig. 13. Again the lack of a complete list of spectral lines at the analysed wavelength region is the major source of the discrepancy between the synthetic and observed spectra. Blend contributions become more important for models with higher T_{eff} and lower abundance of carbon. In these cases carbon abundance determination from the C I lines is rather uncertain.

6.3. τ Her

τ Her was recently investigated by Heasley and Wolff (1981, 1983) by means of the $H\alpha$ and helium line profiles and Strömgren photometry. They obtained $T_{\mathrm{eff}} = 16000$ K, $\log g = 3.8$, and $T_{\mathrm{eff}} = 15000$ K, $\log g = 3.7$ from the non-LTE and LTE analyses, respectively. For our LTE analysis of the C II resonance lines we selected Kurucz's (1979) model with $T_{\mathrm{eff}} = 15000$ K $\log g = 3.5$, whereas Mihalas (1972) model with $T_{\mathrm{eff}} = 15000$ K and $\log g = 4.0$ was used in the non-LTE case. The SWP 3583 image of τ Her near 1335 Å is shown in Fig. 14 together with the calculated spectra for $\xi = 4\ \mathrm{km\,s^{-1}}$ and $V \sin i = 32\ \mathrm{km\,s^{-1}}$ (cf. Hoffleit, 1982), $\log N(\mathrm{C/H}) = -3.63$ (LTE case) and -3.48 (non-LTE

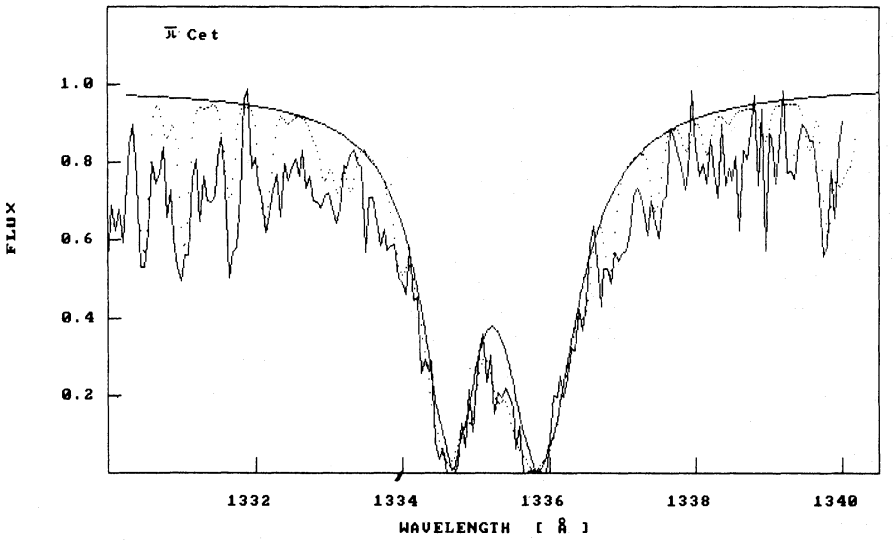

Fig. 12. Comparison of the LTE synthetic spectrum (dots), non-LTE line profiles (solid line) of the C II resonance multiplet with SWP 16246 image of π Cet. The LTE synthetic spectrum was calculated using Kurucz's (1979) model atmosphere with $T_{\mathrm{eff}} = 13000$ K, $\log g = 3.5$, $\xi = 2\ \mathrm{km\,s^{-1}}$, $V \sin i = 18\ \mathrm{km\,s^{-1}}$ and $\log N(\mathrm{C/H}) = -3.63$. The non-LTE line profiles correspond to a Borsenberger and Gros (1978) model atmosphere with $T_{\mathrm{eff}} = 13000$ K, $\log g = 4.0$, $\xi = 2\ \mathrm{km\,s^{-1}}$, $V \sin i = 18\ \mathrm{km\,s^{-1}}$ and $\log N(\mathrm{C/H}) = -3.55$

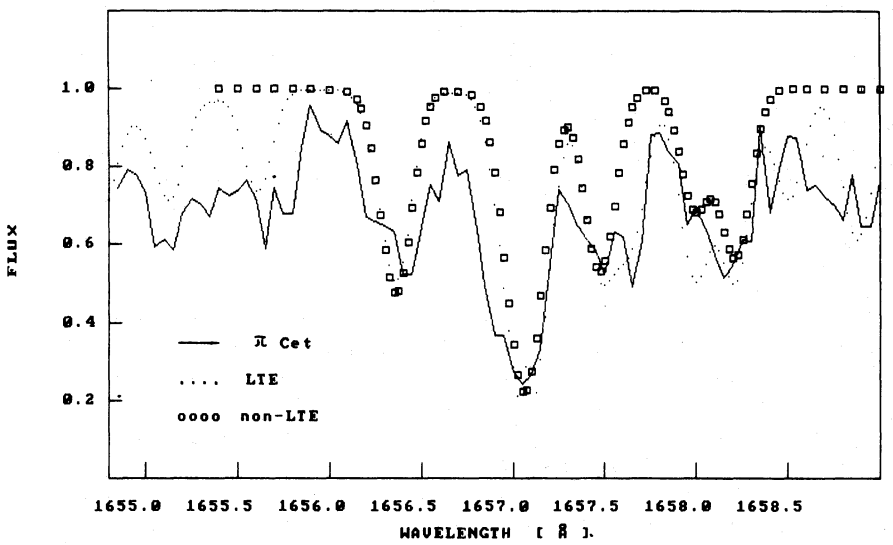

Fig. 13. Comparison of the LTE synthetic spectrum (dots), non-LTE line profiles (squares) of the C I multiplet at 1657 Å with the SWP 16246 image of π Cet (solid line). $\log N(\mathrm{C/H}) = -4.3$ (LTE) and -3.45 (non-LTE) were obtained using model atmospheres as in Fig. 12

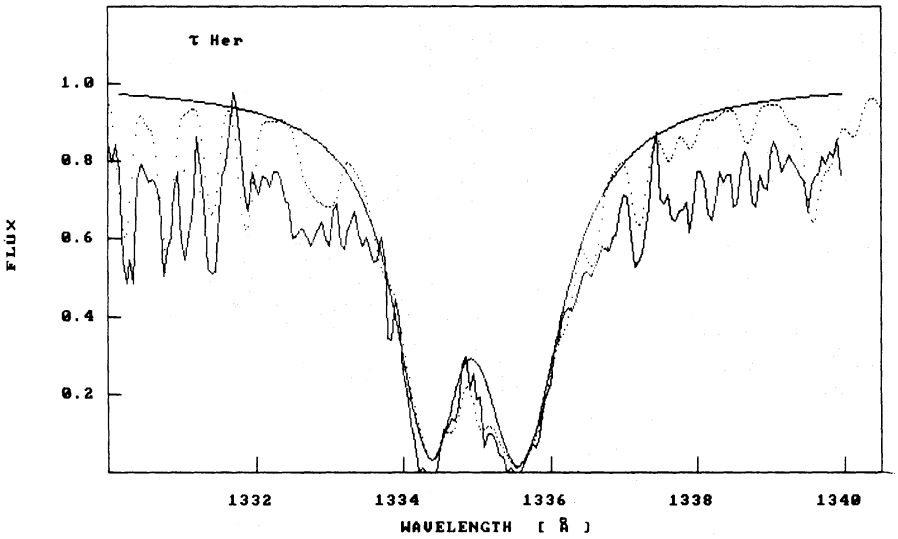

Fig. 14. Comparison of the LTE synthetic spectrum (dots), non-LTE line profiles (solid line) of the C II resonance multiplet with SWP 3583 image of τ Her. The LTE synthetic spectrum was calculated using Kurucz's (1979) model atmosphere with $T_{\rm eff}=15000$ K, $\log g=3.5$, $\xi=4.0\ {\rm km\,s^{-1}}$, $V\sin i=32\ {\rm km\,s^{-1}}$ and $\log N({\rm C/H})=-3.63$. The non-LTE line profiles correspond to a Mihalas (1972) model atmosphere with $T_{\rm eff}=15000$ K, $\log g=4.0$, $\xi=4.0\ {\rm km\,s^{-1}}$, $V\sin i=32\ {\rm km\,s^{-1}}$ and $\log N({\rm C/H})=-3.48$

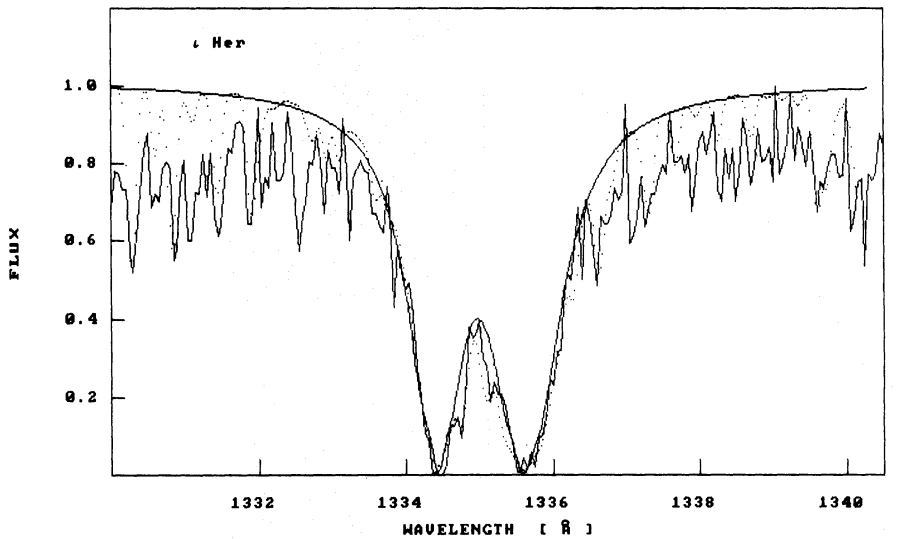

Fig. 15. Comparison of the LTE synthetic spectrum (dots), non-LTE line profiles (solid line) of the C II resonance multiplet with SWP 5720 image of ι Her. The LTE synthetic spectrum was calculated using Kurucz's (1979) model atmosphere with $T_{\rm eff}=18000$ K, $\log g=3.5$, $\xi=1.5\ {\rm km\,s^{-1}}$, $V\sin i=11\ {\rm km\,s^{-1}}$ and $\log N({\rm C/H})=-3.68$. The non-LTE line profiles correspond to a Mihalas (1972) model atmosphere with $T_{\rm eff}=17500$ K, $\log g=4.0$, $\xi=1.5\ {\rm km\,s^{-1}}$, $V\sin i=11\ {\rm km\,s^{-1}}$ and $\log N({\rm C/H})=-3.55$

case), respectively. The final carbon abundances shown in Table 6 were corrected to $\log g=3.7$ of τ Her following the procedure explained at Sect. 4.3.

6.4. ι Her

Figure 15 shows synthetic spectra calculated for the Kurucz's model atmosphere with $T_{\rm eff}=18000$ K, $\log g=3.5$, $\log N({\rm C/H})=-3.68$ (LTE case) and Mihalas (1972) model with $T_{\rm eff}=17500$ K, $\log g=4.0$, $\log N({\rm C/H})=-3.55$ (non-LTE case) together with the SWP 5720 spectrum of ι Her. The model atmospheres used in the analysis were selected according to Heasly and Wolff (1981, 1983). $V\sin i=11\ {\rm km\,s^{-1}}$ (cf. Hoffleit, 1982) and $\xi=1.5\ {\rm km\,s^{-1}}$ were adopted. The final carbon abundances shown in Table 6 were corrected to $\log g=3.7$ of ι Her (see Sect. 4.3).

6.5. α Leo

Code et al. (1976) obtained an empirical effective temperature of α Leo equal to $T_{\rm eff}=12200\ {\rm K}\pm300\ {\rm K}$ by combining observations of the UV flux from OAO-2 satellite and ground-based photometry with the measured angular diameter of the star. We obtained $\log g=3.61$ by making use of the photometric indices of the Strömgren photometry, taken from Lindemann and Hauck (1973). The Kurucz model atmosphere with $T_{\rm eff}=12000$ K and $\log g=3.5$ was selected for the LTE analysis of the C II resonance lines.

In the case of α Leo and other stars with high rotational velocity, calculated synthetic spectra were normalized to the observed ones at wavelength regions which are relatively free from spectral lines. The lack of a complete list of spectral lines included in the calculations may introduce some errors in the interpretation of observed C II line profiles. In order to estimate how this affects the carbon abundance determination, we broadened the observed spectrum of π Cet to the rotational velocity equal to $260\ {\rm km\,s^{-1}}$ and then determined carbon abundance using LTE synthetic spectra. We obtained almost the same value of $\log N({\rm C/H})$ as in the original analysis of π Cet described in Sect. 6.2. A similar procedure, applied to the non-LTE line pro-

files of C II seen in Fig. 12, reveals some discrepancies between the observed and calculated spectra mainly in the far wings, which are caused by the fact that the non-LTE line profiles were obtained without taking into account blends of other elements. Therefore, for stars with high rotational velocities we used LTE synthetic spectra for carbon abundance determinations. The correction equal to -0.11 dex was applied to estimate non-LTE carbon abundances shown in Table 6.

Figure 16 shows the LTE synthetic spectrum calculated for Kurucz's (1979) model atmosphere with $T_{\rm eff}=12000$ K and $\log g=3.5$ in comparison with SWP 19236 image of α Leo. We obtained $\log N({\rm C/H})=-4.43\pm0.20$. The values of $V\sin i=260$ km s^{-1} (cf. Slettebak, 1975) and $\xi=0$ were adopted. A non-zero microturbulent velocity would give only slightly smaller abundance of carbon (cf. Sect. 4).

6.6. 7 Cep

This is a B7 V star with a high $V\sin i$ showing moderate underabundnace of carbon: we obtained $\log N({\rm C/H})=-4.13\pm0.15$ from the LTE analysis of the C II resonance lines. $T_{\rm eff}$ and $\log g$ of 7 Cep listed in Table 1 were obtained from the Strömgren photometry following the procedure explained at Sect. 6.2. Furthermore, the best fit of the LTE synthetic spectrum to the IUE observations shown in Fig. 17 was obtained for $V\sin i=200$ km s^{-1}, which is smaller by about 30% than the value given by Hoffleit (1982).

6.7. ψ^2 Aqr

Among the investigated stars, ψ^2 Aqr shows the weakest C II resonance lines (cf. Sect. 2). We derived $T_{\rm eff}=15100$ K and $\log g=4.0$ from the Strömgren photometry as explained in Sect. 6.2. Kurucz's (1979) model atmosphere with $T_{\rm eff}=15000$ K and $\log g=4.0$ was selected for the analysis of the C II lines, which yielded $\log N({\rm C/H})=-5.0\pm0.2$. The best fit of the LTE synthetic spectrum to the observations of ψ^2 Aqr is shown in Fig. 18. The calculated spectrum was obtained for $V\sin i=280$ km s^{-1} (cf. Slettebak, 1975) and $\xi=0$.

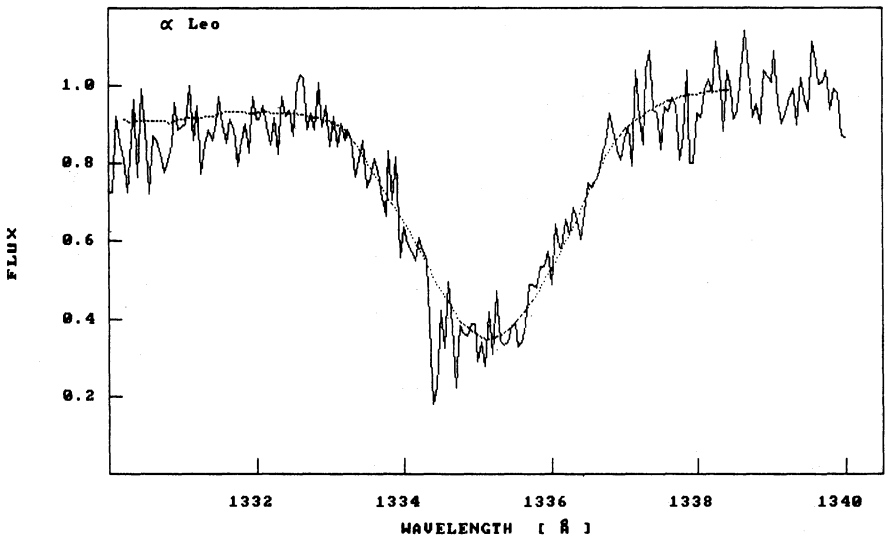

Fig. 16. Comparison of the LTE synthetic spectrum (dots) near the C II resonance multiplet with SWP 16246 image of α Leo. The synthetic spectrum was calculated using Kurucz's (1979) model atmosphere with $T_{\rm eff}=12000$ K, $\log g=3.5$, $\xi=0$, $V\sin i=260$ km s^{-1} and $\log N({\rm C/H})=-4.43$

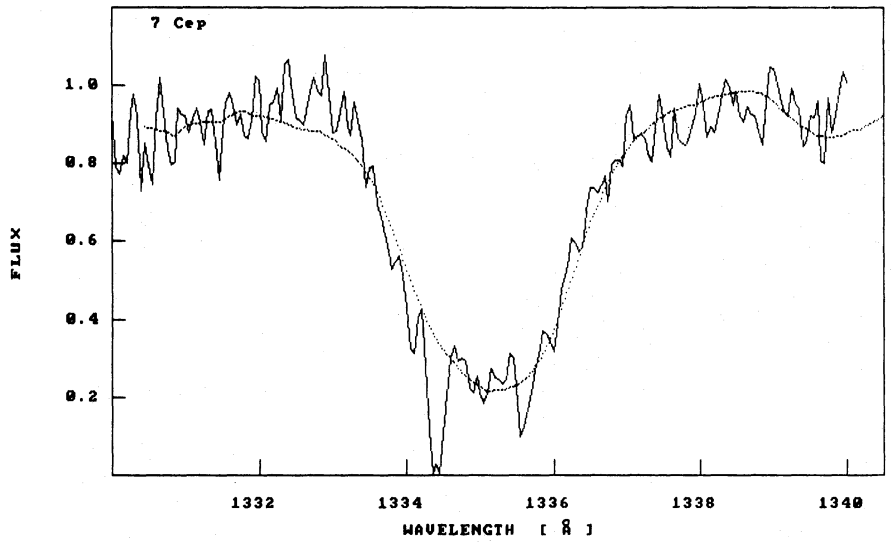

Fig. 17. Comparison of the LTE synthetic spectrum (dots) near the C II resonance multiplet with SWP 8922 image of 7 Cep. The synthetic spectrum was calculated using Kurucz's (1979) model atmosphere with $T_{\rm eff}=13000$ K, $\log g=3.5$, $\xi=0$, $V\sin i=200$ km s^{-1} and $\log N({\rm C/H})=-4.13$

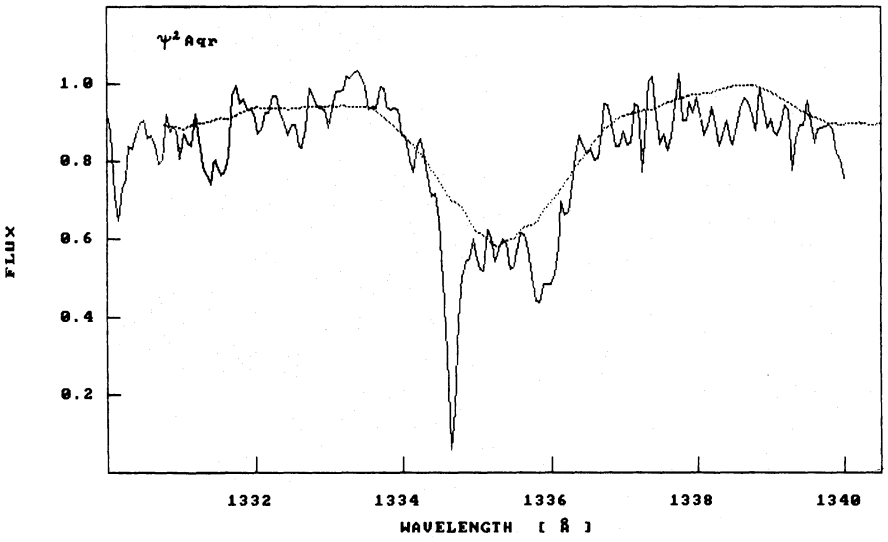

Fig. 18. Comparison of the LTE synthetic spectrum (dots) near the C II resonance multiplet with SWP 10385 image of ψ^2 Aqr. The synthetic spectrum was calculated using Kurucz's (1979) model atmosphere with $T_{\rm eff}=15000$ K, $\log g=4.0$, $\xi=0$, $V\sin i=280$ km s^{-1} and $\log N({\rm C/H})=-5.00$

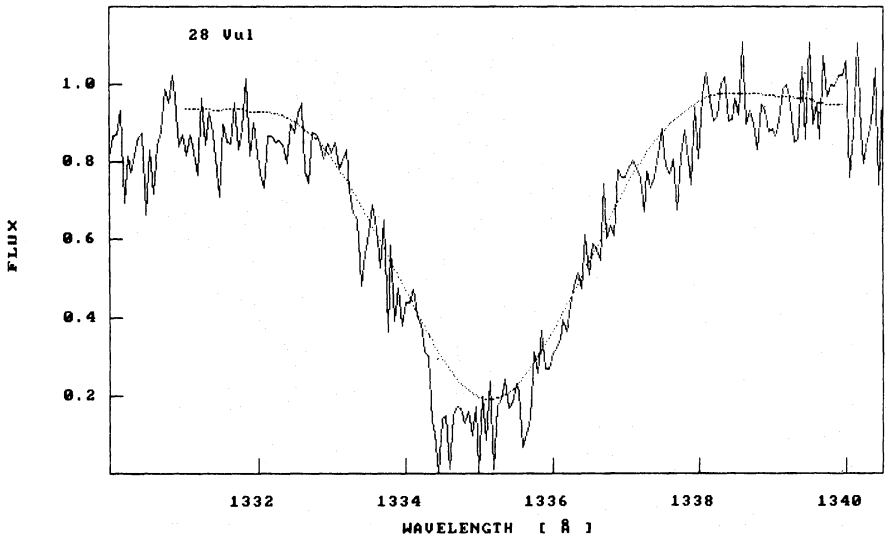

Fig. 19. Comparison of the LTE synthetic spectrum (dots) near the C II resonance multiplet with SWP 18017 image of 28 Vul. The synthetic spectrum was calculated using Kurucz's (1979) model atmosphere with $T_{\rm eff}=15000$ K, $\log g=4.0$, $\xi=0$, $V\sin i=332$ km s^{-1} and $\log N({\rm C/H})=-3.63$

6.8. 28 Vul

As can be seen from Fig. 19, where the observed C II resonance lines are plotted together with the synthetic spectra, 28 Vul is an example of a star with high rotational velocity ($V\sin i=330$ km s^{-1}, cf. Hoffleit 1982) which does not show significant underabundance of carbon. We obtained $\log N({\rm C/H})=-3.63\pm0.15$ in LTE analysis. Kurucz's (1979) model atmosphere with $T_{\rm eff}=15000$ K, $\log g=4.0$ was selected according to the observed Strömgren indices of the star taken from Lindemann and Hauck (1973).

7. Results and discussion

In the present study we have analysed the C II resonance lines at 1335 Å of eight main-sequence stars of spectral types A0V–B3V, using observational data taken from the IUE archives. Remarkably different strengths of the C II lines were found by a direct comparison of the observed spectra of stars with the same atmospheric parameters (Sect. 2). The interstellar components do not influence significantly the observed line profiles and can be easily separated from the stellar spectra in the case of rapid rotators.

In the present analysis we used Kurucz's (1979) grid of model atmospheres in order to calculate the LTE synthetic spectra, whereas Mihalas (1972) and Borsenberger and Gros (1977) models were adopted in the non-LTE case. All calculations were carried out on an IBM/XT Personal Computer with a 10 Mb Hard Disc. The atomic parameters and line broadening mechanisms of the C II resonance multiplet are now known with high accuracy (Sect. 3.1). In the temperature range of interest, carbon is predominantly singly ionized, so that the C II resonance lines vary little with $T_{\rm eff}$ and $\log g$. For model temperatures with $T_{\rm eff}=10000$ to 17500 K, the non-LTE level populations corresponding to this multiplet differ noticeably from the LTE ones only in outer layers where the line cores originate (Sect. 4.2). Finally, partial redistribution effect have some influence on the emergent line profiles (Sect. 4.3). The emergent line profiles tend to be

slightly weaker than those corresponding to the case of complete redistribution. We would like to stress once more that our calculations with partial redistribution were performed for the most simple form of the emission coefficient for the far wings (Sect. 4.3). In particular, we used the approximation of the two-level atom without continuum and neglected the influence of the partial redistribution on non-LTE level populations of carbon.

Both LTE and non-LTE line-profile calculations show that the observed differences in the C II resonance lines reflect carbon abundance differences in the investigated stars. Our final carbon abundance estimates are summarized in Table 6. As one can see from this table, stars with low rotational velocities (Vega, π Cet, τ Her and 1 Her) show $\log N(\mathrm{C/H}) = -3.55$ to -3.45 (in non-LTE case). Substantial differences of carbon abundance were found among the fast rotating stars. ψ^2 Aqr, α Leo and 7 Cep have $\log N(\mathrm{C/H}) = -4.9 \pm 0.2$, -4.32 ± 0.20, and -4.02 ± 0.20, respectively, whereas 28 Vul shows $\log N(\mathrm{C/H}) = -3.52 \pm 0.20$. These results can be compared with the cosmic value of -3.48 given by Allen (1973). The underabundance of carbon in ψ^2 Aqr and α Leo seems to be quite definite on the basis of the comparison of the observed C II line profiles with the calculated synthetic spectra. The same conclusion follows from the direct comparison of the observed spectra of stars with the same atmospheric parameters.

The fact that very different carbon abundances are observed among fast rotating stars favours the possibility that the processes responsible for producing carbon depletion in B-type stars are intrinsic to the stars themselves. Paczynski (1973) has pointed out that the time scale of mixing due to the meridional circulations is significantly shorter than the nuclear time scale in the 3 to 7 $M_\odot$ main-sequence stars with high rotational velocities. For α Leo we estimate the characteristic time scale of mixing to be of the order of (0.8 to 4.0) 10^6 yr, whereas the age of this star should be about (1.2 to 1.6) 10^8 yr. Therefore, meridional circulations, if they exist, may bring up to the stellar surface the products of the CNO bi-cycle of nucleosynthesis. Qualitatively the same results can also be obtained for ψ^2 Aqr and 7 Cep. However, if meridional circulations play a role, a more complicated picture would emerge, because not all fast rotating stars which are evolved from the ZAMS, show significant depletion of carbon, e.g., 28 Vul analysed in this paper.

As far as carbon depletion of ψ^2 Aqr, α Leo and 7 Cep is concerned, it would be interesting to look for other stars of spectral types B7 to B5 V which show underabundance of carbon. For example, there are He-weak Bp stars with low rotational velocities, which show underabundance of helium and carbon together with an excess of He^3 (cf. e.g., Wolff, 1983). An analysis of the He lines may shed some light on the question whether ψ^2 Aqr, α Leo and 7 Cep are members of this group of peculiar stars (but with high rotational velocities).

Acknowledgements. H.C. would like to acknowledge the International Exchange Program SUNY for a partial support during his stay at Stony Brook in 1984/5. The National Space Science Data Center at the NASA Goddard Space Flight Center provided the IUE tapes, Richard Wagner explained the IUE programs at Stony Brook, Dr. M. Jerzykiewicz critically read the manuscript, and the referee, Dr. R. Freire Ferrero, made several useful remarks and comments. To them all we express our thanks. This research was supported in part by NASA through grant NAG 5-555.

References

Adelman, S.J., Leckrone, D.S.: 1986, IUE ESA *Newsletter* **26**, 41
Allen, C.W.: 1973, *Astrophysical Quantities*, Athlone Press, London
Auer, L.H.: 1973, *Astrophys. J.* **180**, 469
Auer, L.H., Heasley, J.N., Milkey, R.W.: 1972, *Kitt Peak National Obs. Contr.* No. 555
Auer, L.H., Mihalas, D.: 1969, *Astrophys. J.* **158**, 641
Auer, L.H., Mihalas, D.: 1970, *Monthly Notices Roy. Astron. Soc.* **149**, 65
Beeckmans, F.: 1977, *Astron. Astrophys.* **60**, 1
Boggess et al.: 1978, *Nature* **275**, 7
Borsenberger, J., Gros, M.: 1978, *Astron. Astrophys. Suppl.* **31**, 291
Code, A.D., Davis, J., Bless, R.C., Hanbury Brown, R.: 1976, *Astrophys. J.* **203**, 417
Crawford, D.L.: 1973, in *Problems of Calibration of Absolute Magnitudes and Temperatures of Stars*, eds. B. Hauck, B.E. Westerlund, Reidel, Dordrecht, p. 93
Dreiling, L.A., Bell, R.A.: 1980, *Astrophys. J.* **241**, 737
Freire Ferrero, R.: 1979, *Astron. Astrophys.* **78**, 148
Freire Ferrero, R., Gouttebroze, P.: 1985, in *Progress in Stellar Spectral Line Formation Theory*, Proc. NATO Adv. Res. Workshop, Trieste, eds. J.E. Beckman, L. Crivellari, Reidel, Dordrecht, p. 125
Freire Ferrero, R., Gouttebroze, P., Kondo, Y.: 1983, *Astron. Astrophys.* **121**, 59
Freudenstein, S.A., Cooper, J.: 1978, *Astrophys. J.* **224**, 1079
Gavrila, M.: 1967, *Phys. Rev.* **163**, 147
Griem, H.R.: 1968, *Phys.* Rev. **165**, 258
Griem, H. R.: 1974, Spectral Line Broadening by Plasmas Academic Press, New York.
Hardorp, J., Cugier, H., Koratkar, A., Scott, J.: 1986, in *Proc. New Insights in Astrophysics—8 Year of UV Astronomy with IUE*, London, U.K.
Hayes, M.A., Nussbaumer, H.: 1984, *Astron. Astrophys.* **134**, 193
Heasley, J.N., Wolff, S.C.: 1981, *Astrophys. J.* **245**, 977
Heasley, J. N., Wolff, S.C.: 1983, *Astrophys. J.* **269**, 634
Henry, R.J.W.: 1970, *Astrophys. J.* **161**, 1153
Henry, R.J.W., Burke, P.G., Sinfailan, A.L.: 1969, *Phys. Rev.* **178**, 218
Herkowitz, M.D., Seaton, M.J.: 1973, *J. Phys. B* **6**, 1176
Hoffleit, D.: 1982, *The Bright Star Catalogue*, 4th edition, Yale University Observ., New Haven, Connecticut, USA
Hofsaess, D.: 1979, *Atomic Data and Nuclear Data Tables* **24**, 285
Hubeny, I.: 1980, *Astron. Astrophys.* **86**, 225
Hubeny, I.: 1981, *Astron. Astrophys.* **98**, 96
Kneer, F.: 1975, *Astrophys. J.* **200**, 367
Kurucz, R.L.: 1970, *Smithsonian Astrophys. Obs. Spec. Rept. No.* 309
Kurucz, R. L.: 1979, *Astrophys. J. Suppl.* **40**, 1
Kurucz, R.L.:1981, *Smithsonian Astrophys. Obs. Spec. Rept. No.* 390
Kurucz, R.L., Avrett, E.H.: 1981, *Smithsonian Astrophys. Obs. Spec. Rept. No.* 391
Kurucz, R.L., Peytremann, E.: 1975, *Smithsonian Astrophys. Obs. Spec. Rept. No.* 362
Lambert, D.L., Roby, S.W., Bell, R.A.: 1982, *Astrophys. J.* **254**, 663
Lennon, D.J., Dufton, P. L., Hibbert, A., Kingston, A. E.: 1985, *Astrophys. J.* **294**, 200

Lindemann, E., Hauck, B.: 1973, *Astron. Astrophys. Suppl.* **11**, 119.
Lotz, W.: 1968, *Z. Phys.* **216**, 241
Loulergue, M., Nussbaumer, H.: 1974, *Astron. Astrophys.* **34**, 225
Milliard, B., Pitois, M.L., Praderie, F.: 1977, *Astron. Astrophys.* **54**, 689
Mihalas, D.: 1972, NCAR, Boulder, NCAR-TN/STR-76
Mihalas, D.: 1978, Stellar Atmospheres, Freeman, San Franciso
Nussbaumer, H., Storey, P.J.: 1981, *Astron. Astrophys.* **96**, 91
Nussbaumer, H., Storey, P.J.: 1984, *Astron. Astrophys.* **140**, 383
Paczynski, B.: 1973, *Acta Astron.* **23**, 191
Peach, G.: 1969, *J. Phys. B.* **1**, 1088
Relyea, L.J., Kurucz, R.L.: 1978, *Astrophys. J. Suppl.* **37**, 45
Sahal-Bréchot, S., Segre, E.R.: 1971, *Astron. Astrophys.* **13**, 161
Seaton, M.J.: 1962, *Atomic and Molecular Processes*, ed. D.R. Bates, New York, Academic Press, p. 374
Slettebak, A.: 1975, *Astrophys. J. Suppl.* **29**, 137
Snijders, M.A.J.: 1977, *Astron. Astrophys.* **60**, 377
Snow, Jr., T.P., Jenkins, E.B.: 1977, *Astrophys. J. Suppl.* **33**, 269
Unsöld, A., Weidemann, V.: 1955, *Vistas Astron.* **1**, 249
Van Regemorter, H.: 1962, *Astrophys. J.* **136**, 906
Vidal, C.R.: Cooper, J. Smith, E.W.: 1973, *Astrophys. J. Suppl.* **25**, 37
Wiese, W.L., Smith, M.W., Glennon, M.: 1966, *Atomic Transition Probabilities*, NSRDS-NBS **4**
Wolff, S.C.: 1983, *The A-Stars: Problems and Perspectives* NASA SP-463 (Washington: NASA, and Paris: CNRS)